Utah State University
DigitalCommons@USU

All Graduate Theses and Dissertations | Graduate Studies

12-2012

Modulation of the Host Response to Tacaribe Arenavirus Infection in AG129 Mice by MY-24

Eric Sefing
Utah State University

Follow this and additional works at: https://digitalcommons.usu.edu/etd

 Part of the Biology Commons

Recommended Citation

Sefing, Eric, "Modulation of the Host Response to Tacaribe Arenavirus Infection in AG129 Mice by MY-24" (2012). *All Graduate Theses and Dissertations*. 1395.
https://digitalcommons.usu.edu/etd/1395

This Thesis is brought to you for free and open access by the Graduate Studies at DigitalCommons@USU. It has been accepted for inclusion in All Graduate Theses and Dissertations by an authorized administrator of DigitalCommons@USU. For more information, please contact digitalcommons@usu.edu.

www.manaraa.com

MODULATION OF THE HOST RESPONSE TO TACARIBE ARENAVIRUS INFECTION IN AG129 MICE BY MY-24

by

Eric Sefing

A thesis submitted in partial fulfillment
of the requirements for the degree

of

MASTER OF SCIENCE

in

Bioveterinary Science

Approved:

_____	_____
Brian B. Gowen Major Professor	E. Bart Tarbet Committee Member
_____	_____
Chris J. Davies Committee Member	Kenneth L. White Department Head

_____

Mark R. McLellan
Vice President for Research and
Dean of the School of Graduate Studies

UTAH STATE UNIVERSITY
Logan, Utah

2012

www.manaraa.com

ABSTRACT

Modulation of the Host Response to Tacaribe Arenavirus Infection in AG129 Mice by MY-24

by

Eric Sefing, Master of Science

Utah State University, 2012

Major Professor: Brian B. Gowen
Department: Animal, Dairy and Veterinary Science

MY-24 is an aristeromycin derivative previously shown to protect AG129 type I and II interferon receptor knockout mice from lethal challenge with Tacaribe virus (TCRV). TCRV is nonpathogenic to humans, but is closely related to the highly pathogenic New World arenaviruses that cause often-fatal viral hemorrhagic fever syndromes. Remarkably, MY-24 prevented mortality without reducing TCRV burden in the circulation or tissues. To investigate the mechanism by which MY-24 protects AG129 mice against TCRV infection, we first characterized the natural history of disease in the model with an emphasis on cytokine responses and vascular integrity to establish the best times to evaluate the effects of MY-24 treatment on host responses believed to contribute to pathogenesis and fatal outcome. We found that viral replication in the blood and in various tissues precedes a hyperproduction of proinflammatory mediators that may lead to the destabilization of the endothelial barrier and increased vascular leakage believed to contribute to terminal shock associated with severe cases of

www.manaraa.com

hemorrhagic fever. We also found slightly reduced virus titers in certain tissues from MY-24-treated mice, suggesting that there may be a weak antiviral effect; however, TCRV was not cleared from lung, spleen, brain or kidney in recovering animals out to 40 days post-infection, indicative of the establishment of chronic infection in mice that are able to survive the initial challenge. Neutralizing antibodies do not appear to play a major role in the antiviral effect of MY-24, whereas reductions in several key proinflammatory cytokines in mice treated with MY-24 may serve to reduce vascular leakage caused by TCRV infection.

www.manaraa.com

PUBLIC ABSTRACT

Modulation of the Host Response to Tacaribe Arenavirus Infection in AG129 Mice by MY-24

by

Eric Sefing, Master of Science

Utah State University, 2012

Major Professor: Brian B. Gowen
Department: Animal, Dairy and Veterinary Science

MY-24 is a new antiviral compound recently shown to protect immunocompromised mice from lethal challenge with Tacaribe virus (TCRV). Tacaribe virus is incapable of causing disease to humans, but is closely related to the highly pathogenic New World arenaviruses that cause often-fatal viral hemorrhagic fever syndromes. Remarkably, MY-24 prevents mortality without reducing virus burden in the circulation or tissues. To investigate the mechanism by which MY-24 protects AG129 mice against Tacaribe virus infection, we first characterized the natural history of disease in the model with an emphasis on host immune response and blood vessel function to establish the best times to evaluate the effects of MY-24 treatment on host immune responses believed to contribute to disease severity and fatal outcome. We found that viral replication in the blood and in various tissues precedes an overzealous immune response that may lead to the destabilization of the blood vessels and increased fluid leakage believed to contribute to fatal shock associated with severe cases of hemorrhagic

www.manaraa.com

fever. We also found slightly reduced virus titers in certain tissues from MY-24-treated mice, suggesting that there may be a weak antiviral effect; however, TCRV was not cleared from lung, spleen, brain or kidney in recovering animals out to 40 days post-infection, indicating the establishment of a chronic infection infection in mice that are able to survive the initial challenge. Neutralizing antibodies do not appear to play a major role in the antiviral effect of MY-24, whereas reductions in several key factors that cause inflammation in mice treated with MY-24 may serve to reduce fluid leakage caused by Tacaribe virus infection.

www.manaraa.com

ACKNOWLEDGEMENTS

I wish there were a way to thank every person who has influenced or helped me along the way during the course of this research. I would, however, like to acknowledge some of the people without whom it would not have been possible. First, the Institute for Antiviral Research and the National Institute of Health for supporting and funding the project. I am very appreciative of my graduate committee, E. Bart Tarbet and Chris Davies, for their invaluable guidance and time. I am especially grateful to Deanna P. Larson for her patience, unfading technical advice and ceaseless encouragement. I would also like to acknowledge all those who helped with practical aspects of the experiments, particularly Brett L. Hurst with his technical knowledge of cytokine analysis and Isaac Wong and his technicians with their assistance in the animal work. A special thank you goes to Stewart W. Schneller of Auburn University for his generous contribution of the MY-24 compound. Finally, I wish to express my gratitude to Brian B. Gowen who provided the guidance and advice throughout this project. Special thanks to you all.

Eric J. Sefing

www.manaraa.com

CONTENTS

Page

www.manaraa.com

LIST OF TABLES

www.manaraa.com

LIST OF FIGURES

www.manaraa.com

CHAPTER 1

INTRODUCTION

1. Arenaviruses - Emerging human pathogens

A group of close to 30 arenaviruses make up the *Arenaviridae* family of viruses [1]. They are a diverse group of enveloped, single-stranded negative sense RNA viruses with bi-segmented genomes, serologically and phylogenetically divided into Old World and New World lineages [2,3]. Novel arenaviruses are being discovered, on average, every 2-3 years, and the recent emergence of new pathogenic arenavirus species is of great concern as these viruses are zoonotic agents harbored in rodent reservoirs with the potential to come in close contact with expanding rural human populations [4,5]. Arenaviruses develop asymptomatic chronic infections in their rodent hosts and can be transmitted to humans by inhalation of aerosolized excreta or contaminated secretions. Transmission from persistently infected rodents to humans can also occur through contact of infectious materials with skin abrasions. Humans infected with arenaviruses develop a wide range of disease signs and symptoms from asymptomatic or mild febrile illnesses that clear within a few days to severe hemorrhagic fever (HF) requiring prompt medical attention. The onset of arenaviral HF proceeds inconspicuously leading to immunosuppression, high viremia, hypercytokinemia, increased vascular permeability, extensive organ damage and eventually hypovolemic shock [6]. There are presently 7 arenaviruses known to cause viral HF. The group includes 5 New World viruses (Junin, Machupo, Guanarito, Sabia, and Chapare) present in areas of South America, and two Old World viruses (Lassa and Lujo) found in defined regions of Western and South Africa [7,8].

www.manaraa.com

The New World arenaviruses (NWA) are comprised of 3 distinct clades, designated clade A, B and C, collectively within the Tacaribe complex [2]. Clade B contains the 5 highly pathogenic arenavirues and several closely related non-pathogenic viruses including Tacaribe virus (TCRV), first isolated in 1956 from a fruit-eating bat (*Artibeus lituratus*) on the island of Trinidad [9]. TCRV is most closely related to Junin virus (JUNV) [7], the etiologic agent of Argentine HF. JUNV has produced the greatest disease burden due to infection by the pathogenic NWA, with case fatality rates ranging from 15-30% in hospitalized patients [10]. Dysregulation of the host innate immune response by JUNV and other pathogenic NWA is believed to impair the development of protective immunity, leading to morbidity and potentially lethal results [6,11]. Those that survive infection develop an antiviral immune response that controls infection with the eventual systemic clearance of the virus.

In addition to being public health concerns from natural transmission in endemic regions of South America, the pathogenic NWA are considered bioterror agents that could be intentionally released in highly populated areas across the globe [12]. While arenaviruses are a concern to the health and safety to the human population in close contact with the natural rodent reservoirs harboring the highly pathogenic clade B arenaviruses, the aerosol transmissibility of these viruses makes them serious biothreats. Further, the lack of safe and effective therapeutic options also contributes to the designation of JUNV and other HF-causing NWA as highest priority category A NIAID pathogens [12]. The only proven effective vaccine against an arenavirus HF is the JUNV Candid #1 attenuated virus vaccine [13]. However, the vaccine is only indicated for

www.manaraa.com

those at high risk in the endemic regions of Argentina, such as agricultural workers and those that live near areas prone to infestation by the rodent host, *Calomys musculinus* [14]. Currently, Immune plasma is considered the standard of treatment for Argentine HF; however, the lack of efficacy in clinical disease past 8 days of evolution, the risk of transfusion associated diseases, and difficulties of maintaining sufficient stockpiles of immune plasma support continued drug development efforts [10].

The Old World arenaviruses [15] include the prototypical arenavirus, lymphocytic choriomeningitis virus (LCMV), a medically important arenavirus particularly in immune compromised individuals, and Lassa virus (LASV), by far the arenaviral HF agent that has caused the greatest morbidity and mortality. LCMV infections generally cause mild febrile illness sometimes associated with aseptic meningitis, but can also cause severe disease in fetuses or newborns [16]. Organ transplant patients are also at higher risk of productive infection and have high mortality during outbreaks of LCMV [17]. Lassa Fever, the most significant arenaviral disease in terms of number of cases, was first described during a 1969 outbreak in Nigeria [18]. LASV is endemic to Western Africa and afflicts approximately 300,000 people with an estimated 5000 deaths annually [19]. In endemic regions of Western Africa, LASV infection causing severe disease results in mortality rates of >15%, with up to 50% case fatality in hospital acquired infections [20,21]. More recently, Lujo virus emerged in Southern Africa with the index case and 3 of the 4 caregivers exposed to the virus succumbing to the infection (80% lethality) [5]. The only survivor was treated with ribavirin, but it is not clear whether the intervention had a significant effect on the outcome of that fifth case. In patients with severe Lassa fever, ribavirin has been shown to have some efficacy in treating disease within the first

www.manaraa.com

six days of evolution [22]; however, previously noted side effects that include hemolytic anemia are less than desirable when treating a disease where hemorrhaging can be significant [23]. Nevertheless, ribavirin is considered the standard of care in Western Africa for treating severe LASV infections [24], and in the US in the event of a bioterrorist act, an imported case, or laboratory accident [12].

2. Arenavirus molecular and cell biology

Genetic diversity is considerable among the *Arenaviridae* family members, even within the same virus species. Despite the genetic variability at the nucleotide and amino acid levels, there are common features shared by all arenaviruses. Arenavirus virions are generally pleomorphic particles ranging from 50-300 nm in diameter and contain electron dense ribosomal particles, which under an electron microscope give the virus a grainy appearance [25]. Consequently, the family name “arena” is derived from the Latin term “arenosus” which means “sandy” [25]. The arenaviruses are non-lytic and replicate strictly in the cytoplasm. The genome consists of two single stranded ambisense RNA segments encoding 4 proteins [26]. The large (L) and small (S) viral RNA segments each include two open reading frames in mutually opposite orientations separated by a noncoding intergenic region with a predicted stable hairpin structure [26]. The S segment is 3.4 kb in length and encodes the viral nucleoprotein and glycoprotein precursor (GPC) which is post translationally cleaved to form GP1 and GP2 [27]. The L segment is 7.2 kb in length and encodes the viral RNA-dependent RNA polymerase (L protein) and a matrix (Z) protein [28]. In addition to its polymerase function, L also has 5’ endonuclease activity for “cap-snatching”. The GPC and Z matrix proteins are translated from subgenomic virus sense mRNA, while the nucleoproteins and RNA polymerase are

www.manaraa.com

translated from subgenomic virus anti-sense mRNA. NP, Z and L are translated in the cytosol while the viral GPC is a type I membrane protein synthesized in the host cell's secretory pathway [29].

NP is the major structural protein encapsidating the viral genome and also has cap-binding activity to assist L-mediated viral replication and transcription [30]. The NP associates with viral RNA to form nucleocapsids [15]. The L protein is also incorporated into the viral nucleocapsid [31,32]. The GPC protein is initially synthesized as a single polypeptide cleaved during processing in the endoplasmic reticulum into two glycoproteins, the N-terminal GP1 domain and a transmembrane GP2, by a host cell protease [27,33]. GP1/GP2 forms a tripartite complex with a stable signal peptide (SSP), which represents the arenavirus functional unit for host cell attachment and entry [34]. The GPC is dependent upon the SSP for proper maturation, transport, and membrane fusion [1].

The ability of clade B arenaviruses to cause disease has been directly linked to GP1 binding to transferrin receptor 1 (TfR1) [35], the principal receptor mediating attachment and entry of the NWA that cause HF [36]. Within clade B, only the pathogenic arenaviruses utilize human TfR1, whereas nonpathogenic relatives such as TCRV and Amapari virus recognize the TfR1 ortholog in their respective rodent hosts [37]. The major receptor for clade C and OWA has been found to be α-dystroglycan [38,39]. The receptor for the clade A arenaviruses has not been elucidated.

Once the binding of pathogenic NWA to TfR1 is initiated, the virion is endocytosed and GPC-mediated fusion of the viral and endosomal membranes is activated in response to a change to low pH of the maturing endosome [1]. Clade A and B NWA enter the cell

www.manaraa.com

through clathrin-mediated endocytosis while OWA (LASV and LCMV) entry is independent of clathrin [40]. Once penetration into the cytoplasm occurs the viral ribonucleoprotein acts as a template for transcription and replication mediated by the viral polymerase [41]. Viral transcription and replication is dependent on the L and NP proteins while delayed expression of the Z protein demonstrates a dose dependent inhibitory effect on these processes [31,42,43]. The Z matrix protein is essential to arenavirus budding while the physical interaction of GP and Z is required for the incorporation of GPs into arenavirus virion particles [44]. The formation of the virion particles and the budding of these infectious progeny from infected host cells requires the assembled RNP to associate at the host cell surface enriched with viral GP. The endosomal sorting complex required for transport of RNP components are recruited by the GP and Z interaction to facilitate virion assembly and release from the infected host cell [45] In addition to its critical role in virion egress, the Z protein has been shown to interfere with the type I IFN response [46].

3. Animal models of arenaviral hemorrhagic fever

Proof-of-concept studies utilizing animal models that recapitulate the features of human disease are essential to advance development of promising therapeutic agents towards practical clinical applications. For HF arenaviruses, the greatest challenge has been the lack of disease models in immune competent mice. The currently available infection models are shown in Table 1.

www.manaraa.com

Table 1. Animal Models for the Study of Arenaviral HF

Virus	Disease	Animal model	Selected references
Lassa	Lassa fever	Rhesus macaque	[47], [48], [49]
		Cynomolgus macaque	[50], [51], [52]
		Marmoset	[53]
		Guinea pig	[54], [55]
	Lassa virus replication	HHD[a] mouse	[56]
		MHC-I$^{-/-b}$ mouse	[56]
Lujo	Hemorrhagic fever	Guinea pig	[57]
LCM	Hemorrhagic fever	Rhesus macaque	[58]
		Guinea pig	[59]
Pichinde	Hemorrhagic fever	Guinea pig[c]	[60], [61], [62]
		Hamster	[63], [64], [65]
Pirital		Hamster	[66], [67]
Junin	Argentine hemorrhagic fever	Rhesus macaque	[68], [69]
		Marmoset	[70], [71]
		Guinea pig	[72], [73], [74]
		AG129[d] mouse	[75]
Tacaribe		AG129[d] mouse	[76]
Machupo	Bolivian hemorrhagic fever	Rhesus macaque	[77], [78], [79]
		Cynomolgus macaque	[78]
		African green monkey	[80], [81]
		Guinea pig	[82]
		STAT-1$^{-/-e}$ mouse	[83]

www.manaraa.com

Guanarito	Venezuelan hemorrhagic fever	Guinea pig	[84]
Flexal	Hemorrhagic fever	Hamster	[85]

[a] Genetically engineered mouse that expresses a human/mouse-chimeric HLA-A2.1 molecule in place of the murine MHC-I.

[b] β2-microglobulin-deficient mouse (MHC-$I^{-/-}$).

[c] Virus adapted to produce lethal disease.

[d] Type I and II interferon receptor-deficient mouse.

[e] Signal transducer and activator of transcription 1-deficient mouse (STAT-$1^{-/-}$).

Lymphocytic choriomeningitis, LCM.

Work with most of the arenavirus HF models (Lassa, Lujo, Junin, Machupo, and Guanarito) is restricted to approximately 6 biosafety level (BSL-4) maximum containment laboratories in the US, and several facilities abroad. Accessibility to such labs and the high cost associated with conducting studies in BSL-4 has limited research in this area. Although more accessible and less biohazardous, the use of Pichinde (BSL-2), Pirital (BSL-2), and Flexal (BSL-3) clade A arenavirus models is less than ideal considering that all the HF NWA are in clade B. To this end, we developed a model based on the challenge of AG129 mice with the clade B TCRV, a virus that can be worked with safely in BSL-2 containment [76].

In addition to its relatedness to JUNV, TCRV can be adapted to produce dramatic cytopathic effect (CPE) making it amenable to use in high-throughput screening (HTS) *in vitro* for identification of small molecule inhibitors that could be useful against the pathogenic clade B relatives. Compounds identified by this approach that demonstrated antiviral activity and specificity against TCRV were also found to be active against JUNV and other pathogenic clade B NWA in other cell culture-based assays [86]. The

www.manaraa.com

lead compound, ST-294, was further evaluated in a previously described newborn BALB/c mouse model [87]. Effective treatment following TCRV challenge of 4-day-old BALB/c mice by the intraperitoneal (i.p.) route provided proof-of-concept that ST-294 had activity *in vivo* [86]; however, the difficulty of working with newborn animals prompted others to pursue other alternatives. This lead to the development of the AG129 IFN-α/β and γ receptor-deficient mouse TCRV challenge model [76]. This model has been particularly useful in evaluating promising anti-arenavirus compounds that have little to no activity against the clade A Pichinde virus (PICV) *in vitro*. Until the development of the TCRV model, only animal studies in hamsters challenged with PICV could be performed in BSL-2, requiring both activity against PICV and far greater quantities of compound, which are often limited in early stages of drug discovery and development. In addition, work with the apathogenic TCRV greatly reduces the risks associated with arenavirus research. The inability of TCRV to antagonize the host interferon response like other NWA likely contributes to its lack of pathogenicity [88].

4. Small molecule experimental therapies for treatment of arenaviral infections

While there is an expanding list of compounds that have demonstrated anti-arenaviral activity *in vitro*, most have not been evaluated in experimental animal models [8], and, thus, are beyond the scope of this literature review. There are, however, several promising small molecules that have shown efficacy in several of the models described in section 3. ST-294 is potent and selective compound that was effective in the newborn TCRV mouse challenge model; however, activity was restricted to clade B NWA [86]. A second compound with expanded spectrum, ST-193, was found to be protective against

www.manaraa.com

the LASV infection in strain 13 guinea pigs [89]. The ST compounds represent a new class of viral entry inhibitors that disrupt the interaction between the GP2 subunit and the SSP [90,91]. With its broad-spectrum activity against both Old and NWA, ST-193 is the most promising lead for further development. Because it has a mechanism of action distinct from ribavirin [1,92], combination therapy studies testing ST-193 and ribavirin in guinea pig or nonhuman primate models of arenaviral HF should be considered.

Favipiravir (T-705) is a compound originally described as a potent influenza virus inhibitor [93,94], and has advanced through clinical trials in Japan for the treatment of influenza virus infections. The compound is presently in phase II clinical trials in the US for the same indication. In addition to its activity against influenza, several laboratories have shown that the compound broadly inhibits RNA virus infections [95]. If approved for use against influenza virus, favipiravir could be used "off-label" for other viral diseases including arenaviral HF, as the compound has been shown to inhibit multiple arenaviruses including JUNV [96]. Favipiravir acts like a purine nucleoside analog inhibiting the influenza virus RNA dependent RNA polymerase, and the polymerase is also the likely arenavirus target [96,97]. Remarkably, favipiravir has been shown to be active against advanced PICV infection even when delaying treatment until after the onset of clinical disease [98,99]. Encouraging results have fueled further development of favipiravir as a therapeutic for the treatment of JUNV infection in guinea pigs, and ultimately nonhuman primates.

As a result of *in vitro* screening efforts, our lab identified MY-24, an aristeromycin derivative, as an inhibitor of TCRV in a series of cell culture screening assays. Because the compound was also found to be active against the attenuated Candid #1 vaccine strain

www.manaraa.com

of JUNV, it was evaluated in the TCRV AG129 mouse infection model [76]. In those experiments, MY-24 consistently protected close to 100% of treated mice from lethal challenge with TCRV. Most impressive was the fact that therapy was still effective even when delaying the initiation of MY-24 treatment as late as 5 days post infection [76]. Remarkably, however, treatment did not significantly reduce virus titers, suggesting that the beneficial protective effect may be due to amelioration of the pathogenesis related to an overzealous host response. The current thinking is that excessive production of inflammatory mediators triggers vascular leak, and ultimately hypovolemic shock is the cause of death in severe cases of viral HF [100,101].

At present, it is unclear how MY-24 is protecting TCRV-challenged mice from mortality. The compound is an analog (5'-homoaristeromycin) of aristeromycin, a carboxylic nucleoside antibiotic that has been shown to inhibit AMP synthesis in mammalian cells and most importantly, in the context of antiviral research, has demonstrated inhibition of the enzyme S-adenosylhomocysteine hydrolase (AdoHcyase) [102,103]. AdoHcyase catalyzes the hydrolysis of S-adenosylhomocysteine to form adenosine and homocysteine products that are crucial in the methylation process associated with various biological processes, including RNA capping [104]. Because of toxicity from 5'-phosphate formation, aristeromycin has not advanced in development as an antiviral agent [105,106]. In contrast, MY-24 is far less toxic than aristeromycin, and was well tolerated in mice. Despite having anti-TCRV activity in cell culture, the compound does not appear to act in a similar fashion in mice, as reduced titers were not evident. Thus, we hypothesize that the MY-24 is reducing hypercytokinemia elicited in response to TCRV infection, and thereby limiting vascular leak and its putative

www.manaraa.com

contribution to the demise of the AG129 mice.

www.manaraa.com

CHAPTER 2

MATERIALS AND METHODS

1. Animals

Six- to seven-week-old AG129 IFN-α/β and -γ receptor-deficient mice were used in these experiments and were obtained from the breeding colony at USU. They were fed irradiated mouse chow and autoclaved water *ad libitum*.

2. Ethics statement

All animal procedures complied with USDA guidelines and were conducted at the AAALAC-accredited Laboratory Animal Research Center at Utah State University (USU) under protocol 1425 approved by the USU Institutional Animal Care and Use Committee.

3. Virus

TCRV, strain TRVL 11573, was obtained from American Type Culture Collection (ATCC; Manassas, VA). The virus stock ($10^{6.35}$ 50% cell culture infectious doses ($CCID_{50}$)/ml) was prepared from clarified liver homogenates from AG129 mice challenged with TCRV (2 passages in Vero 76 African green monkey kidney cells). Virus stock was diluted in sterile MEM plus 50 μg/ml gentamicin and inoculated by bilateral i.p. injections totaling 0.2 ml.

4. Natural history of disease in AG129 mice challenged with TCRV

Mice were sorted based on age and gender into 9 groups of 4 animals per group,

www.manaraa.com

and 1 group with 5 mice to account for projected deaths late in the course of infection. The animals were ear tagged and individual weights were determined every other day starting on day 0 relative to the time of virus infection with approximately 450 $CCID_{50}$ of TCRV. Groups of 4 TCRV-infected animals were sacrificed daily, with 1 of the 5 mice in the day-10 group succumbing prior to sacrifice. Ten sham-infected mice (normal controls) were included in the study for daily sacrifice [one per day] and comparison to the TCRV-challenged animals. Serum and liver, spleen, brain, kidney, and lung tissues were obtained for virus titer determination and cytokine profiling. The spleens from all animals were weighed prior to processing for virus titers. Whole blood collected in EDTA-coated tubes was analyzed for hematology using the VetScan HMT (Abaxis Inc. Union City, CA). A sample of each tissue was preserved in 10% formalin and sent to the Ross A. Smart Veterinary Diagnostic Laboratory (VDL; Logan, UT) for histopathology. Here and elsewhere, clarified tissue homogenates in minimal essential medium and serum were stored at -80 °C until time of analysis.

5. Tissue virus titer determinations

Virus titers were assayed using an infectious cell culture assay as previously described [96]. Briefly, a specific volume of tissue homogenate or serum was serially diluted and added to triplicate wells of Vero 76 (African green monkey kidney) cell

www.manaraa.com

monolayers in 96-well microtiter plates. The viral cytopathic effect (CPE) was determined 7-8 days post-virus inoculation, and the titers were calculated by endpoint titration [96]. The assay detection ranges were 2.8 - 9.5 $\log_{10}$ $CCID_{50}$/g of tissue or 1.8 - 8.5 $\log_{10}$ $CCID_{50}$/ml of serum. In samples presenting with undetectable tissue or serum virus, a value of < 2.8 or 1.8 $\log_{10}$ was assigned, respectively. Therefore, the mean virus titer for samples with undetectable levels of virus is likely an overestimate of the actual viral load. For statistical analysis, values of 1.8 or 2.8 $\log_{10}$ were assigned for samples with undetectable virus levels.

6. Assessment of vascular leakage

Vascular permeability was determined by intravenous administration of Evans blue dye (EBD) (Sigma-Aldrich, St. Louis, MO) and tracking its diffusion into various tissues as previously described . At designated times following infection, untreated or treated mice were anesthetized with isoflurane and injected retro-orbitally with a 0.5% EBD phosphate-buffered saline (PBS) solution. Retro-orbital injections were given using a 27-guage needle by carefully inserting the tip approximately 1 mm from the outermost edge of the eye into the membrane exposed by gently pulling the skin away from the eye. Once the membrane has been penetrated, the EBD is slowly injected into the eye for absorption by the capillary nexus at that site. After a 3 h period, blood was collected by cheek bleed, and the animals were extensively transcardially perfused with PBS. Similar sized sections of liver, spleen, lung, and kidney tissues were harvested, placed in pre-weighed 1.5 ml microtubes for weight determination, and 0.5 ml of formamide was added for complete immersion of all samples. The EBD was extracted from tissue samples by overnight incubation at 37 degrees C. A 0.2 ml volume from each tube was placed into a

www.manaraa.com

96-well microtiter plate and the absorbance at 610 nm was measured. Relative EBD content in the serum was determined from 1:10 diluted samples measured at 610 nm and 740 nm. The absorbance at 740 nm was subtracted from the 610 nm absorbance values to remove contributions due to hemoglobin contamination. Data are expressed as a ratio of absorbance/g of tissue:absorbance of a 10-fold dilution of serum sample.

7. Compounds.

MY-24 was provided by Stewart Schneller (Auburn University, Auburn, AL). The synthesis of the compound has previously been reported [107] and its *in vitro* and *in vivo* activity against TCRV has been described [76]. MY-24 was dissolved in sterile saline solution and administered by i.p. injection.

8. MY-24 mechanism of action studies

Mice were sorted based on age for males and weight for females into 6 TCRV infected groups of 5-6 animals per group. The animals were ear tagged and individual weights were determined every third day. Animals were treated with saline vehicle placebo or 25 mg/kg of MY-24, once daily for up to 8 days starting 3 days post-challenge with ~450 $CCID_{50}$ of TCRV. Groups of 5 MY-24- and placebo-treated mice were sacrificed on day 8, and remaining 4-5 mice per group on days 16, 24, 32 and 40 relative to time of infection. Placebo-treated animals were not included for these later time points because they would not be expected to survive the TCRV challenge. Five sham-infected normal control mice were included in the study for sacrifice at the different time points and comparison to the TCRV-challenged animals. Serum and liver, spleen, brain, kidney, and lung tissues were collected for analysis, as described above. Due to death prior to

www.manaraa.com

time of sacrifice, 1 of 5 animals in the 24- and 32-day groups, and 2 of 6 animals in the 40-day group were not included in the analysis. Day-8 samples were assayed for neutralizing antibody titers and profiled for systemic cytokine expression. Spleen samples collected on day 8 were also included in the cytokine analysis.

9. Cytokine multiplex profiling

Tissue and serum concentrations of 16 cytokines (IL-1α, IL-1β, IL-2, IL-3, IL-4, IL-5, IL-6, IL-9, IL-10, IL-12, MCP-1, IFN-γ, TNF-α, MIP-1α, GM-CSF, and RANTES) were evaluated in TCRV-infected mice using Q-Plex mouse cytokine arrays (BioLegend, San Diego, CA) as recommended by the manufacturer. Samples from normal control animals were included to establish baseline cytokine concentrations in AG129 mice. For the natural history study, fold change was calculated relative to the normal control values (n=3-6) for the respective cytokines. For the experiment to determine the effects of MY-24 treatment on cytokine induction in infected mice, data are presented as pg/ml of serum or pg/g of spleen tissue.

10. Serum plaque reduction and neutralization (PRNT) titers

Neutralizing antibody titers were determined by standard PRNT assay. Briefly, 6-well cell culture plates were seeded with Vero 76 cells to achieve ~70-80 % confluence. Equal volumes of media containing ~400 $CCID_{50}$ of TCRV was added to serial 2-fold dilutions of heat-inactivated (56°C for 30 min) serum samples diluted in MEM supplemented with 2% FBS. Experimental samples were diluted 1:5 to 1:160. The immune serum control was diluted starting at 1:250. The serum plus TCRV mixture was incubated at 37°C for 2 h. After removing media from cells, 200 µl of the serum-TCRV

www.manaraa.com

mixtures were added to respective wells of 6-well plates and incubated at 37°C for 2 h, while rocking plates every 10 min to prevent drying of cells and to distribute virus evenly. After the 2-h absorption period, each well was washed twice with 1 ml of DPBS prior to the addition of a warmed solution of 2 ml of 2% sea plaque agarose (Lonza, Rockland, ME) and an equivalent amount of 2X MEM/4% FBS/gentamicin. Plates were incubated 5 min at 4°C to solidify agarose, and then incubated at 37°C for 6 days, at which time 1 ml filtered-sterilized 0.034% neutral red solution was added to each well and incubated an additional 2 h. Neutral red was aspirated and plaques enumerated with the aid of a light box. Plates were further incubated overnight at 37°C and read on day 7 to verify accuracy of initial plaque count. The neutralizing antibody titers were expressed as the highest dilution of serum reducing the average number of plaques present in the virus control wells (TCRV incubated with normal serum) by 50% or greater ($PRNT_{50}$).

11. Statistical analysis

For analyzing differences in viral titers, cytokine levels, plaque reduction neutralization titer and vascular permeability, one-way analysis of variance [108] with Newman-Keuls posttests were performed. The Mann-Whitney test (two-tailed) was used for evaluating differences in spleen weights and hematology. All statistical evaluations were done using Prism (GraphPad Software, CA).

www.manaraa.com

CHAPTER 3

RESULTS

1. Natural history of TCRV-infection in AG129 mice

One of the goals of the present study was to determine the kinetics of viral replication of TCRV in AG129 mice, as part of a more comprehensive characterization of the infection model. As seen in Figure 1, all tissues examined harbored virus. Virus first became apparent systemically on day 6 in 2 of 4 challenged mice, and titers gradually increased until reaching mean levels above 7.25 $\log_{10}$ $CCID_{50}$/ml on day 9 (Figure 1A). Liver virus was barely detectable in a single animal on day 6, rising to 7.75 $\log_{10}$ $CCID_{50}$/g by day 9 (Figure 1B). By gross visual examination, liver samples taken from day 10 mice were a pale light color in 2 of the 4 survivors. Substantial lung virus titers could be detected in 75% of the mice on day 7, with increasing burden thereafter, reaching peak levels (~6.75 $\log_{10}$ $CCID_{50}$/g) on day 10 (Figure 1C). Gross visual examination of lungs revealed necrotic lesions on day 9 and thereafter. The first organ to present with significant amounts of TCRV replication was the spleen, with >4.75 $\log_{10}$ $CCID_{50}$/g on day 5 of the infection, and sustained virus burden of >6.5 $\log_{10}$ $CCID_{50}$/g out to day 10 (Figure 1D). In several spleen samples collected on and after day 8, gross examination revealed pyogranulomatous lesions and a pale light coloration, in addition to splenomegaly. TCRV was found in the brain in 1 of 4 animals on day 8 and all infected animals thereafter, with up to 6 $\log_{10}$ $CCID_{50}$/g present on days 9 and 10 (Figure 1E). Substantial kidney virus was not observed until day 8 of infection, with the highest mean viral loads of >6.5 $\log_{10}$ $CCID_{50}$/g seen on days 9 and 10 (Figure 1F).

www.manaraa.com

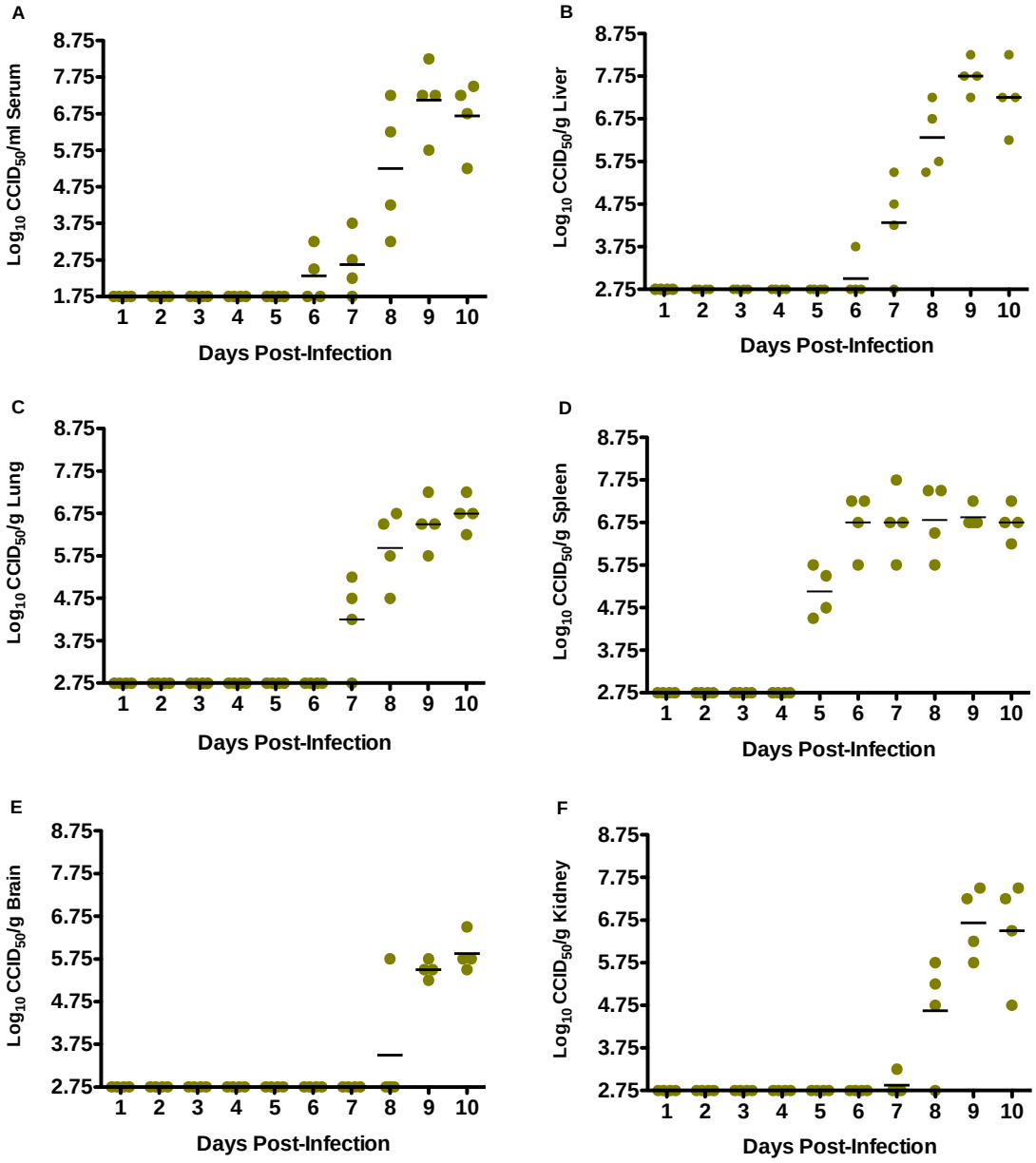

Figure 1. Temporal Analysis of Serum and Tissue Virus Titers in AG129 Mice Challenged with TCRV. Groups of 4 animals were sacrificed on the specified days of infection for analysis of A) serum, B) liver, C) lung, D) spleen, E) brain, and F) kidney virus titers. One of 5 mice in the day-10 group succumbed prior to the time of sacrifice.

www.manaraa.com

The mean weight of the TCRV-infected mice dropped sharply after day 6 (Figure 2). Splenomegaly was also observed as early as day 6 in infected mice, with spleens doubling in weight compared to the sham controls (Figure 3). WBCs increased precipitously starting on day 8, as did the lymphocyte and granulocyte populations (Table 2). Monocytes were slightly increased, also starting on day 8. Notably, platelet counts did not decrease in the TCRV-infected animals (Table 2), which is a characteristic feature of South American hemorrhagic fever [101]. No other significant changes were seen in the hematologic analysis.

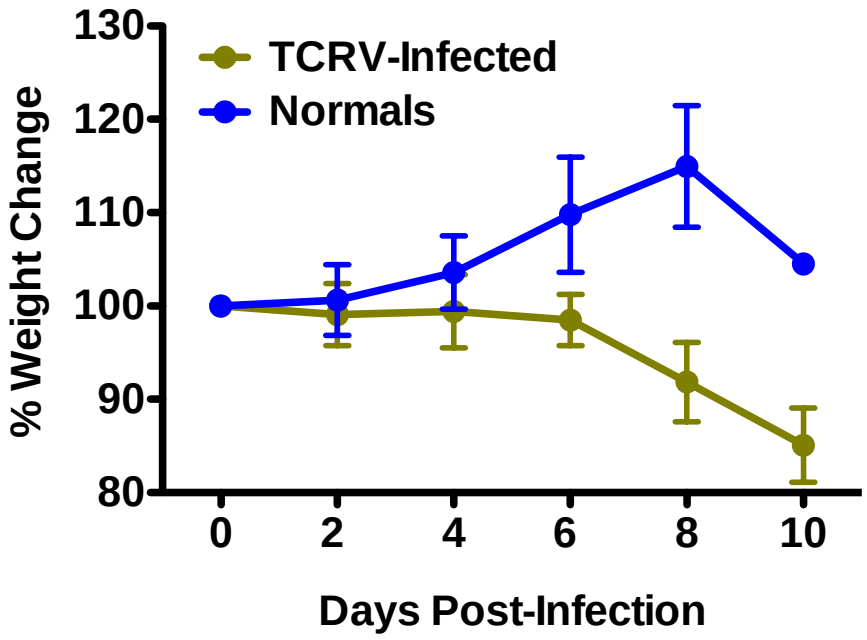

Figure 2. Weight Change in AG129 Mice during the Course of TCRV-Infection. The data are represented as the group mean and standard deviation of the percent change in weight of surviving animals relative to their starting weights, measured at 3-day intervals. n=40, 36, 28, 20, 12, and 4 for the TCRV-infected mice, and n=10, 9, 7, 5, 3, and 1 mouse for the normal controls, on day 0, 2, 4, 6, 8, and 10, respectively.

www.manaraa.com

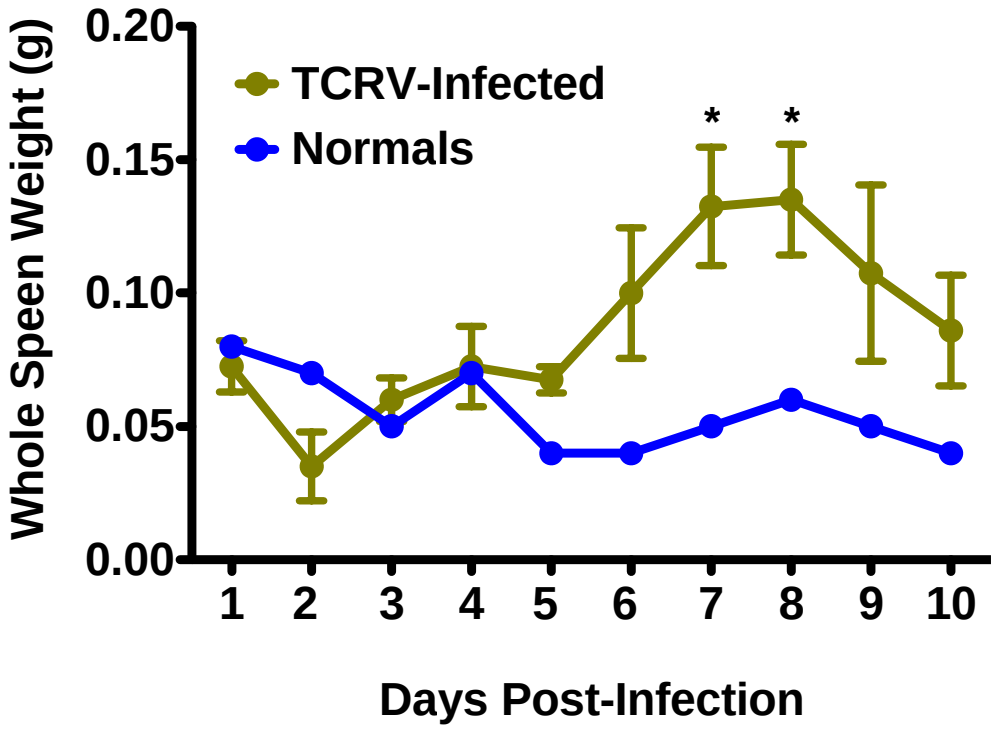

Figure 3. Spleen Weights from Infected AG129 Mice during TCRV-Infection. The data represent the mean and standard deviation from groups of 4 TCRV-infected mice sacrificed at the indicated times. Data from 1 normal control animal per day are included for comparison. *$P < 0.05$ compared to day 1 TCRV infected animals.

www.manaraa.com

المنارة للاستشارات

Table 2[a]. Hematology Analysis in TCRV-Infected AG129 Mice from Days 1 to 10 Post-Infection.

Blood component (units)	Day post-infection									
	1	2	3	4	5	6	7	8	9	10
WBC (m/mm^3)	9.8 ± 1.2	6.4 ± 0.6	12.4 ± 2.1	8.7 ± 1.6	13.8 ± 5.8	10.5 ± 3.3	10.6 ± 5.6	38.2 ± 23.0*	59.9 ± 31.4*	96.9 ± 31.2*
Lym (m/mm^3)	5.2 ± 0.6	4.2 ± 0.6	8.4 ± 1.7	8.3 ± 0.6	7.1 ± 2.8	3.4 ± 1.2	4.3 ± 2.1	14.3 ± 5.8*	14.7 ± 5.6*	14.9 ± 2.7*
Mon (m/mm^3)	1.2 ± 0.4	0.6 ± 0.3	1.2 ± 0.4	0.7 ± 0.3	0.6 ± 0.3	0.6 ± 0.2	0.7 ± 0.3	1.8 ± 0.5	1.5 ± 0.5	1.9 ± 0.2
Gra (m/mm^3)	3.0 ± 1.1	1.7 ± 0.2	2.8 ± 0.7	2.7 ± 1.2	6.2 ± 3.5	6.4 ± 2.3	5.4 ± 3.2	22.3 ± 16.8*	43.8 ± 26.5*	80.2 ± 32.2*
RBC (m/mm^3)	9.4 ± 0.1	9.7 ± 0.1	9.1 ± 0.7	8.7 ± 0.4	9.4 ± 0.6	9.2 ± 0.6	9.7 ± 0.4	9.4 ± 0.4	9.4 ± 0.4	9.6 ± 0.5
MCV (fL)	61.6 ± 2.7	57.8 ± 3.3	60.2 ± 3.7	59.0 ± 1.9	59.0 ± 1.8	59.5 ± 2.5	59.5 ± 3.0	56.4 ± 3.9	57.6 ± 0.9	56.3 ± 1.1
HCT (%)	57.7 ± 2.6	56.0 ± 3.8	55.0 ± 5.7	51.1 ± 1.7	55.2 ± 4.1	55.1 ± 5.9	55.5 ± 4.7	52.9 ± 4.9	54.1 ± 2.7	54.6 ± 1.8
MCH (pg)	17.4 ± 0.1	17.6 ± 0.6	17.9 ± 0.3	17.5 ± 0.3	18.6 ± 2.0	17.4 ± 0.5	17.3 ± 0.3	17.1 ± 0.4	17.4 ± 0.5	17.5 ± 0.3
MCHC (g/dl)	9.9 ± 0.3	9.7 ± 0.3	9.9 ± 0.5	9.9 ± 0.6	10.3 ± 0.4	10.1 ± 0.7	9.3 ± 0.2	10.2 ± 0.7	10.2 ± 0.4	10.3 ± 0.9
RDW	9.3 ± 0.5	10.0 ± 1.1	9.7 ± 0.7	10.1 ± 0.6	9.4 ± 0.8	9.2 ± 0.3	8.8 ± 0.5	9.3 ± 0.2	9.2 ± 0.6	8.6 ± 0.4
Hb (g/dl)	16.3 ± 0.2	17.0 ± 0.4	16.4 ± 1.1	15.2 ± 0.6	17.5 ± 2.9	16.1 ± 0.9	16.7 ± 0.9	16.1 ± 0.7	16.4 ± 1.0	16.9 ± 0.9
PLT (m/mm^3)	70.5 ± 12.4	64.5 ± 23.6	68.8 ± 31.5	61.8 ± 46.8	81.5 ± 31.8	66.8 ± 14.3	53.5 ± 28.5	67.3 ± 10.7	72.3 ± 22	72.3 ± 5.1
MPV (fL)	7.4 ± 0.2	7.4 ± 0.4	7.1 ± 0.3	7.0 ± 0.1	7.2 ± 0.6	7.2 ± 0.4	7.4 ± 0.4	7.6 ± 0.4	7.9 ± 0.5	7.9 ± 0.4
PCT (%)	0.05 ± 0.02	0.05 ± 0.02	0.05 ± 0.02	0.05 ± 0.03	0.06 ± 0.02[e]	0.05 ± 0.02	0.04 ± 0.02	0.05 ± 0.01	0.06 ± 0.02	0.06 ± 0.01
PDW	4.4 ± 5.1	2.5 ± 5.1	4.0 ± 4.7	1.5 ± 3.0	5.8 ± 4.0	4.2 ± 4.8	3.8 ± 4.4	2.4 ± 4.8	4.8 ± 5.7	4.0 ± 4.9

[a] Groups of AG129 mice (n=4) were sacrificed daily through the course of TCRV infection and whole blood was collected for hematologic analysis.

WBC, white blood cells; Lym, lymphocytes; Mon, monocytes; Gra, granulocytes; RBC, red blood cells; MCV, mean corpuscular volume; HCT, hematocrit; MCH, mean corpuscular hemoglobin; MCHC, mean corpuscular hemoglogin concentration; RDW, red cell distribution width; Hb, hemoglobin; PLT, platelets; MPV, mean platelet volume; PCT, plateletcrit; and PDW, platelet distribution width.

*$P < 0.05$

www.manaraa.com

Cytokine levels were examined on days 5-10 in serum, brain and lungs, days 4-10 for kidney, days 3-10 for spleen, and days 2-10 for liver. As shown in top left panel of Figure 4, serum concentrations of IL-6, IL-10, IFN-γ, and MIP-1α in were increased >50-fold as TCRV progressed. Levels of TNF-α and MCP-1 also increased over time, and, in addition to IL-6, have been associated with severe disease in cases of viral hemorrhagic fever [101]. Overall, the cytokines included in the analysis were broadly induced in spleens from infected mice (Figure 4, lower left panel). Notably, however, IL-6, MCP-1, IFN-γ, and MIP-1α, actually demonstrated a trend of induction over time, whereas the concentrations of most other cytokines fluctuated relative to the levels observed in uninfected mice.

Cytokine expression in the livers from infected animals were less remarkable than the high levels observed in the sera and spleen, with temporal induction observed with MCP-1 and MIP-1α, and consistently high levels of IFN-γ (Figure 4, top center panel). In lung tissues, increased production in numerous cytokines was observed later in the course of infection (days 9 and 10) (Figure 4, top right panel). A temporal pattern of increasing concentrations of IL-6, IL-10, MCP-1, IFN-γ, MIP-1α, and RANTES was evident. In general, cytokine production in kidney and brain tended to be suppressed by TCRV infection (Figure 4, bottom right panels).

Although there was histopathology present in spleens by day 7 (Appendix, Table A1), evidence of disease was not seen in other tissues until day 8 of infection. Typical liver lesions included moderate numbers of portal lymphocytes and histiocytes (Figure 5A) and scattered degenerate/necrotic hepatocytes surrounded by small numbers of neutrophils or lymphocytes.

www.manaraa.com

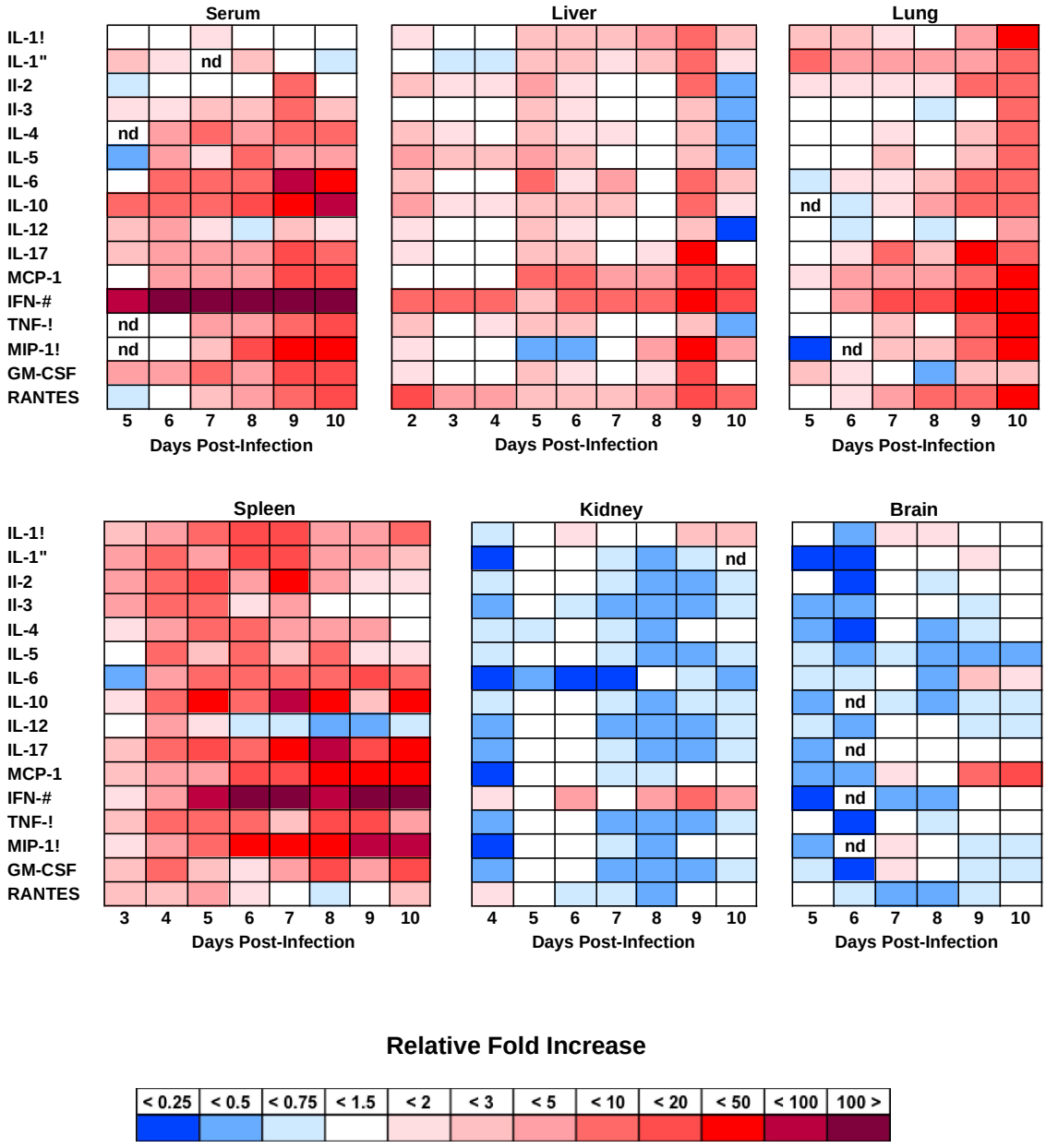

Figure 4 . Cytokine and Chemokine Response to TCRV-Infection. Groups of 4 TCRV-infected animals were sacrificed on the indicated day relative to the time of infection and the serum and tissue concentrations of selected cytokines were determined using a multiplexed array including the indicated cytokines. Fold change in expression is relative to normal animals (n=3-6). In certain cases, cytokines were not detected (nd) in serum or tissue homogenates.

www.manaraa.com

Spleens of infected mice had hyperplastic follicles, follicular lympholysis and increased numbers of interstitial neutrophils (Figure 5B). Findings from day-9 and 10 livers and spleens had similar pathology to that described for day-8 tissue samples (Appendix, Table A1). There was no kidney or brain histopathology associated with advanced TCRV infection in the AG129 mice. Lung histopathology was mild to non-existent on day 8, with the most profound histopathology observed on day 9 (Appendix, Table A1).

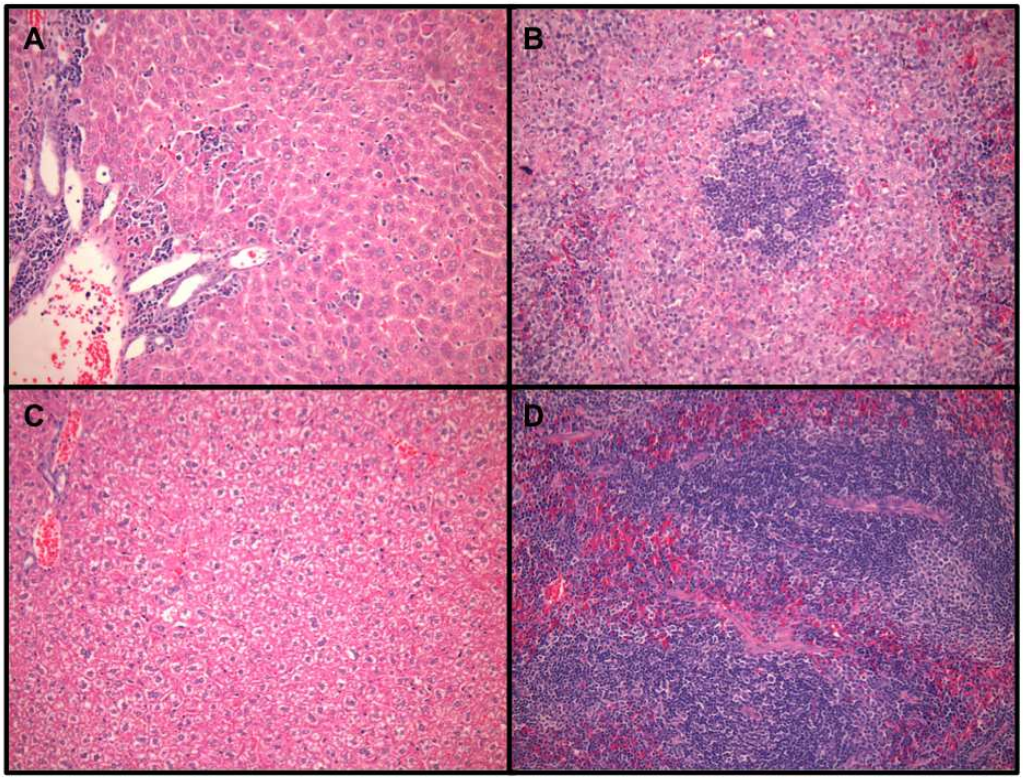

Figure 5. Histologic Examination of Liver and Spleen Sections from TCRV-Infected AG129 Mice. Representative A) liver and B) spleen histopathology on day 8 of TCRV infection in AG129 mice. C) Liver and D) spleen tissue from healthy sham-infected mice. Tissue sections were stained with hematoxylin and eosin.

www.manaraa.com

If we are to consider therapeutic strategies aimed at maintaining vascular integrity in order to limit capillary leakage that ultimately results in plasma volume loss, multi-organ failure and shock, we must first establish that vascular hyperpermeability results from TCRV infection in the AG129 mouse infection model. Thus, we also performed a separate time course analysis of vascular permeability during TCRV infection in AG129 mice by tracking the movement of retro-orbitally injected EBD into various primary tissues. In this study, TCRV-challenged mice exhibited clear signs of clinical illness including lethargy and ruffling of fur by day 8 and 9, and the deteriorating condition of the animals was reflected in loss of body weight (Figure 6). By day 10, the infected mice were approaching a moribund state and the animals that were the most morbid did not show markedly blue extremities as seen in the normal controls or less ill mice (not shown). This is consistent with previously observed lack of perfusion in a model of acute arenavirus infection in hamsters, likely due to hypotension associated with vascular leak [65].

When measuring systemic EBD levels, serum concentrations were reduced in the TCRV-infected control animals on day 8, 9 and 10, suggesting leakage of the dye into the viscera (Figure 7A). However, we cannot rule out the possibility that the lower systemic EBD levels seen at advanced stages of illness in the TCRV-infected mice may be due to lack of absorption from the orbital capillary nexus. Therefore, to more accurately access vascular leak of EBD, the tissue concentrations were normalized to amount of dye present in the serum. Liver, kidney, lung and spleen showed a markedly higher average of tissue to serum ratio in the TCRV-infected animals compared to the sham-infected

www.manaraa.com

mice on day 8, 9 and 10 (Figure 7B-E), indicating that vascular leakage is occurring and may be an important factor in the demise of the AG129 mice challenged with TCRV.

www.manaraa.com

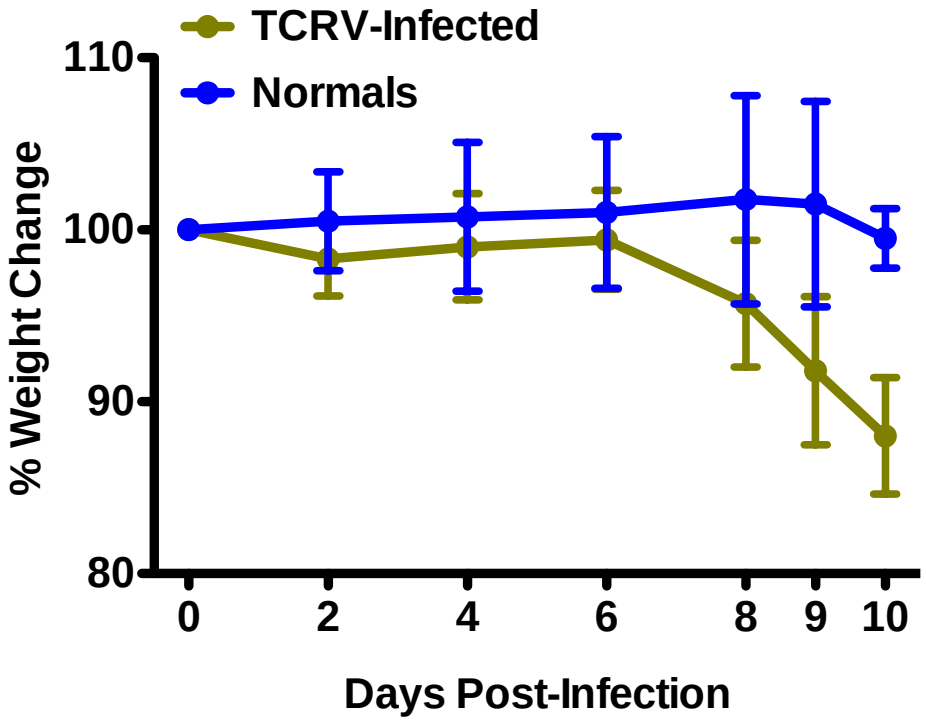

Figure 6. Individual Animal Body Weight Change During the Course of the Vascular Permeability Study. TCRV- and sham-infected mice in the vascular leakage study were weighed on day 0, 2, 4, 6, 8, 9, and 10 post-infection. The data are presented as the group mean and standard deviation of the percent change in weight of surviving animals relative to their starting weights.

www.manaraa.com

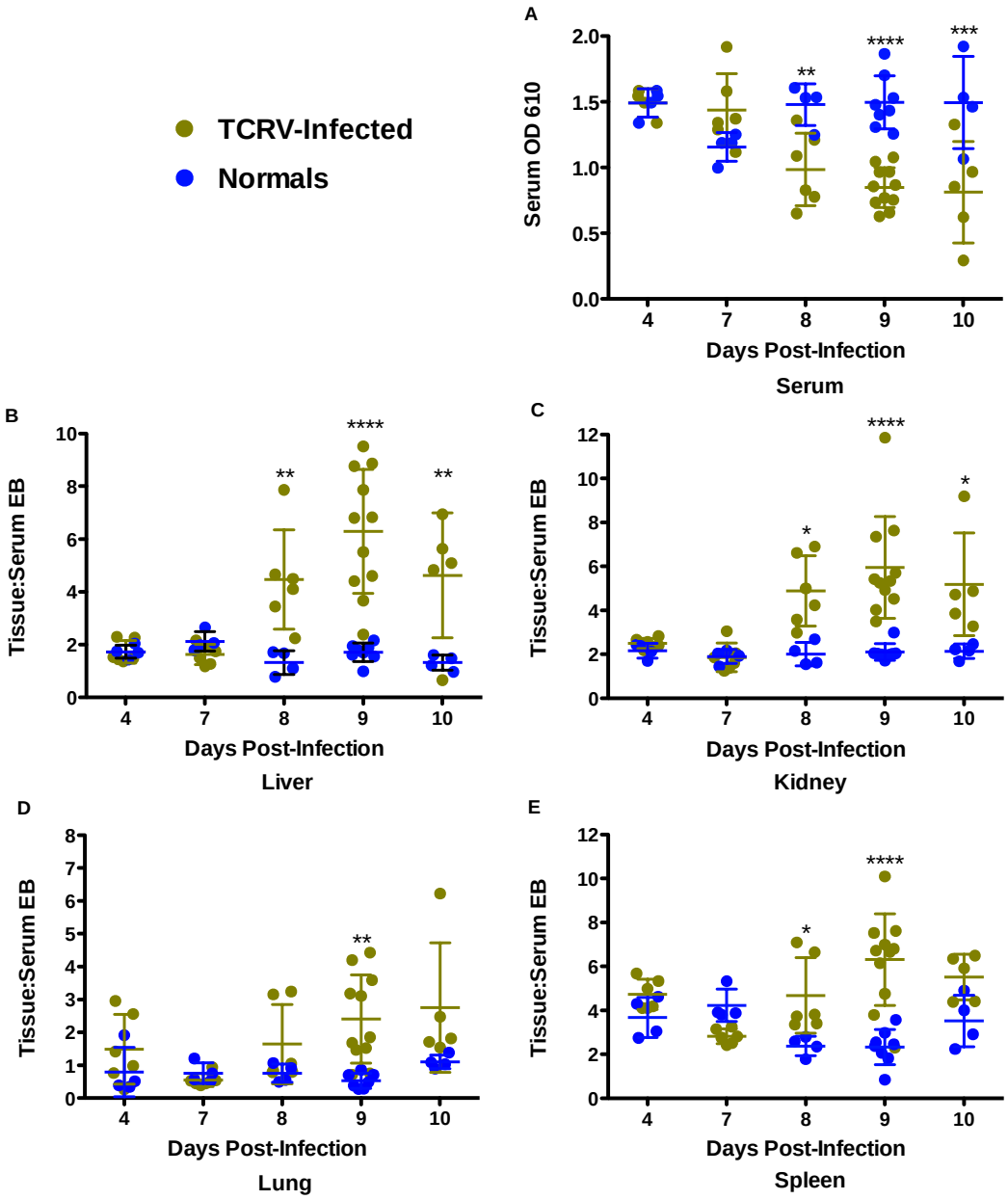

Figure 7. Evaluation of Vascular Permeability During TCRV-Infection in AG129 Mice. TCRV- and sham-infected mice were infused with EB dye on day 4, 7, 8, 9 and 10 of infection and systemic levels, as well as leakage into the viscera was evaluated. A) Serum EB dye levels and ratios of tissue to respective serum levels are shown for B) liver, C) kidney, D) lung, and E) spleen tissues. Day 9 data include values from two separate experiments. *$P < 0.05$, ** $P < 0.01$, *** $P < 0.001$, **** $P < 0.0001$ compared to sham-infected animals.

www.manaraa.com

2. Characterization of the protective effect of MY-24 during TCRV- infection in AG129 mice

The second aim of this study was to measure the ability of MY-24 to clear TCRV from the circulation and tissues in surviving animals successfully treated with the compound. Groups of TCRV-challenged mice treated with 25 mg/kg/day MY-24 were sacrificed on days 8, 16, 24, 32 and 40. Placebo-treated mice were included for the day-8 comparison. On day 8 of the infection, 3 of the 5 MY-24- and placebo-treated mice had detectable virus loads in the serum (Figure 8A). All mice were viremic on day 16, but TCRV was no longer detectable by 24 days in the MY-24-treated mice. As seen with the serum, virus titers in the liver were slightly higher in the placebo-treated animals on day 8 (Figure 8B). Peak viral loads of ~7.5 $\log_{10}$ $CCID_{50}$/g of liver were observed on day 16. The virus was detected in only 2 of 4 surviving animals on day 24 and was cleared by day 32. In the lung, a slight increase in day 8 virus titers was also noted in mice receiving placebo relative to those treated with MY-24 (Figure 8C). Approximately 7 $\log_{10}$ $CCID_{50}$/g of lung was detected on day 16, with a gradual decline in titers out to day 40. Remarkably, >5 $\log_{10}$ $CCID_{50}$/g of tissue virus burden was still present at the end of the 40-day experiment. The spleen was the only tissue in which the viral titers were higher in the MY-24-treated animals on day 8 (Figure 8D). Remarkably, 3 of the 5 MY-24-treated mice had >9.5 $\log_{10}$ $CCID_{50}$/g. Spleen viral burden decreased on days 16-40, but persisted similar to that observed in the lung. On day 8 of the infection, virus was found only in brain tissue from a single placebo-treated animal (Figure 8E). However, substantial titers were observed starting on day 16 ranging from 6 to 7.5 $\log_{10}$ $CCID_{50}$/g of brain. TCRV persistence was also observed in the kidneys of recovering MY-24-treated mice (Figure 8F). As in most tissues, peak titers were

www.manaraa.com

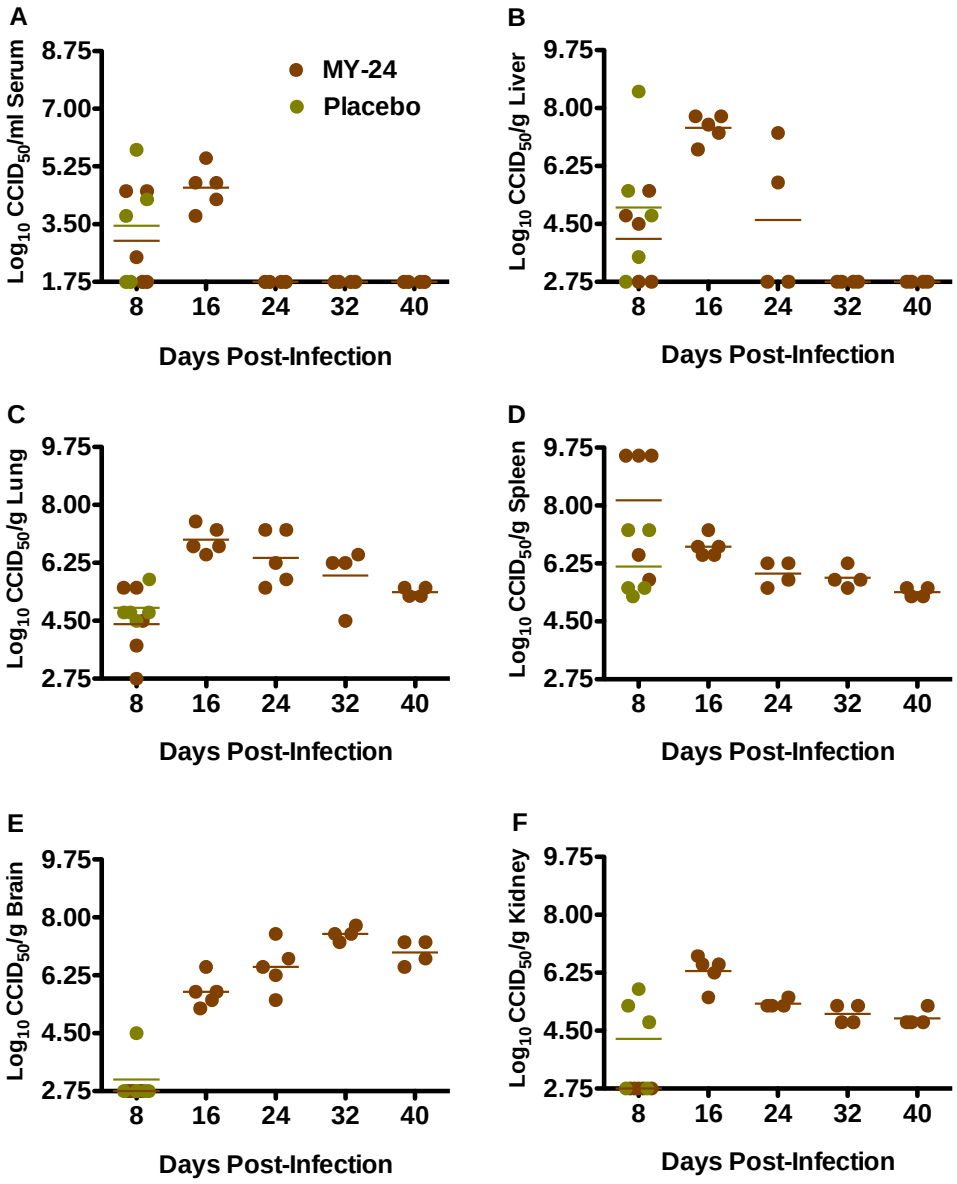

Figure 8. Analysis of Serum and Tissue Virus Titers in AG129 Mice Infected with TCRV and Treated with MY-24. Groups of 4-5 TCRV-infected animals treated with MY-24 or placebo for up to 8 days starting on day 3 post-challenge, were sacrificed on the specified days of infection for analysis of A) serum, B) liver, C) lung, D) spleen, E) brain, and F) kidney virus titers. One mouse per MY-24 group at the 24, 32, and 40 h time points succumbed prior to the time of sacrifice.

www.manaraa.com

observed on day 16 (~6.5 $\log_{10}$ $CCID_{50}$/g of kidney), with a subsequent reduction in titers as the experiment progressed. Notably, 60% (3 of 5) of mice that received placebo had considerable day 8 viral titers, whereas none of the animals treated with MY-24 had detectable virus until day 16. In general, MY-24-treated mice began to lose weight after day 15 and started to recover the lost weight 6 days later (Figure 9). These data are consistent with peak titers being observed primarily on day 16, with reductions in load in most cases by day 24 (Figure 8).

In addition to assessing the viral titers out to 40 days post infection, we also analyzed neutralizing anti-TCRV titers. The day-8 comparison data indicate that low levels of neutralizing antibodies were elicited more quickly in placebo-treated animals (Figure 10). By day 16, $PRNT_{50}$ titers were at their peak in the MY-24-treated mice and waned thereafter. Compared to the $PRNT_{50}$ titers from immune serum from mice that were boosted with live TCRV having survived infection with a non-lethal challenge dose, the primary neutralizing antibody response was relatively weak.

To further gauge the effect of MY-24 treatment on the immune response during TCRV infection in AG129 mice, a multiplex cytokine array analysis was conducted. Cytokine levels were examined on day-8 serum and spleen samples from treated mice and normal controls to assess the impact of MY-24 on systemic inflammation and locally in the spleen. As shown previously in the natural history study (Figure 4), serum IFN-γ was highly stimulated by TCRV infection (Figure 11, top panel). Most notably, however, systemic IL-6 concentration was reduced significantly in MY-24-treated mice. The only other significant difference was a

www.manaraa.com

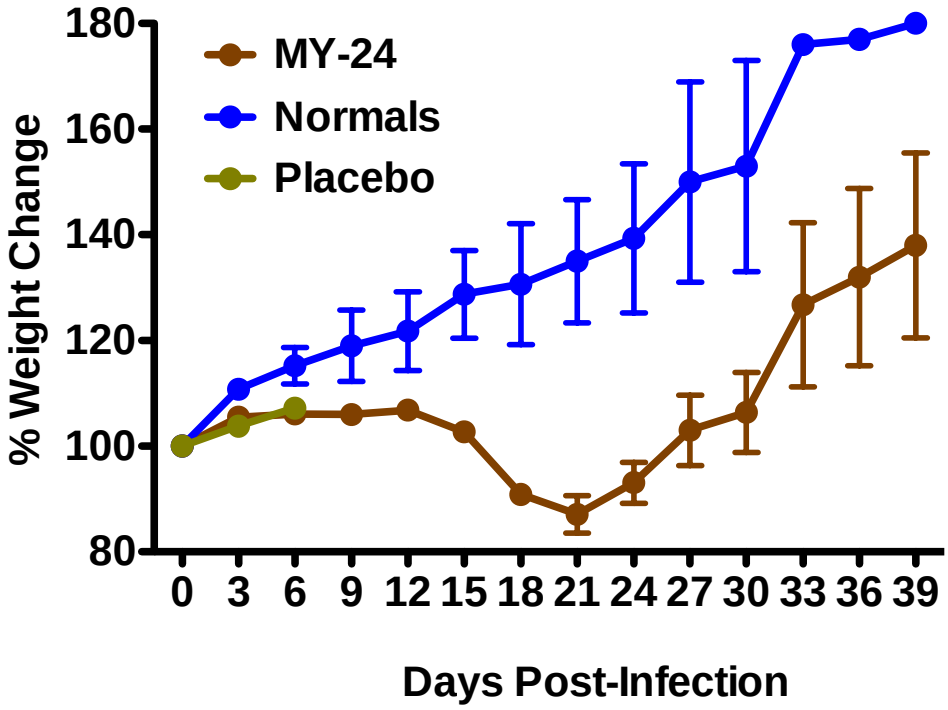

Figure 9. Analysis of Weight Change in AG129 Mice Infected with TCRV and Treated with MY-24 or Placebo. Mice from the longitudinal study described in Figure 8 were weighed every third day over the course of the experiment. Normal control mice (n=5, with 1 mouse each sacrificed on days 8, 16, 24, 32, and 40) are included for comparison. The data are represented as the group mean and standard deviation of the percent change in weight of surviving animals relative to their starting weights.

www.manaraa.com

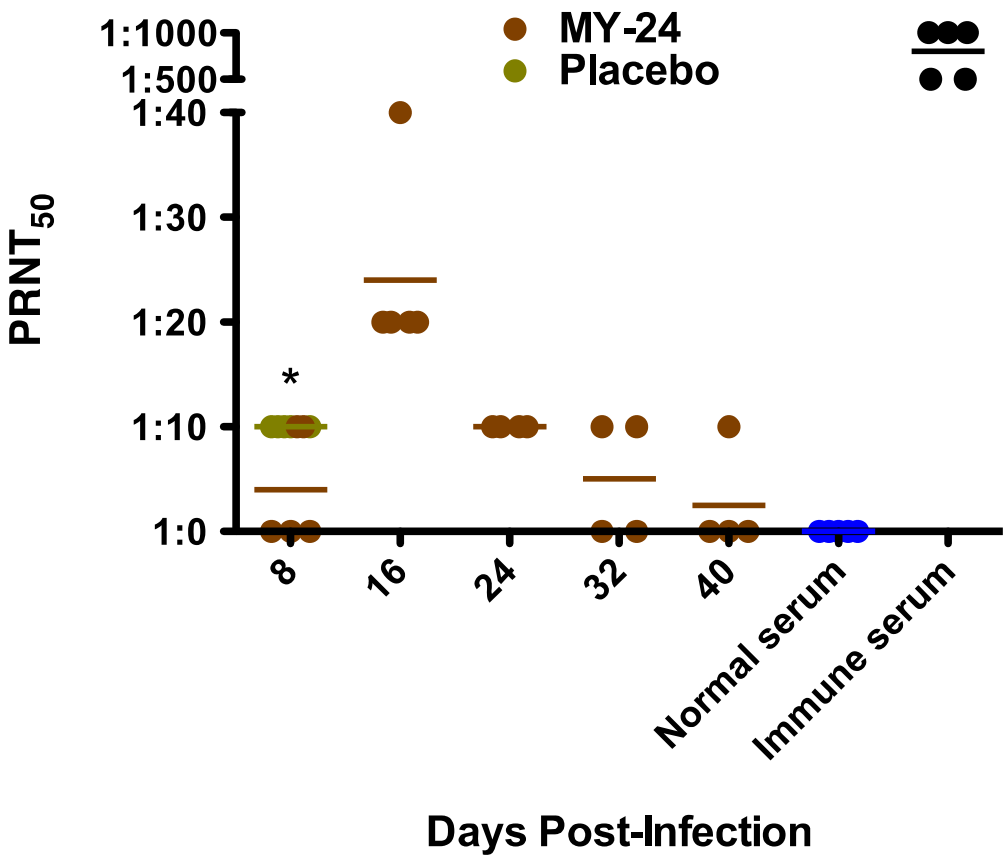

Figure 10. Neutralizing Antibody Levels During the Course of TCRV-Infection and Recovery in AG129 Mice Treated with MY-24. Serum samples from TCRV-infected animals treated with MY-24 or placebo, as indicated in the longitudinal study described in Figure 8, were analyzed for neutralizing antibodies by PRNT. Normal serum from uninfected mice and immune serum were included as controls. *$P < 0.05$.

www.manaraa.com

slightly reduced level of IL-1α observed in the placebo group relative to MY-24 and normal control animals (Figure 11, upper panel). Although not statistically significant, MY-24 also appeared to reduce the levels of TNF-α and MCP-1 (Figure 11, lower panel), which in addition to IL-6, are linked to more severe forms of viral hemorrhagic fever [101].

Consistent with the natural history data, IFN-γ, MIP-1α, and MCP-1 were clearly induced in the spleens 8 days after TCRV infection (Figure 12). RANTES was the only cytokine significantly altered by the MY-24 treatment (Figure 12, upper panel). Unlike the trend of higher serum cytokine concentrations in the placebo-treated animals (Figure 11), greater levels of most cytokines and chemokines were observed in MY-24 treated animals (Figure 12). This may be a reflection of the higher splenic virus titers in mice treated with MY-24 (Figure 8D). It is conceivable that this more robust immune response locally is preferable, in contrast to systemic inflammation that can trigger vascular leakage.

Based on the natural history study, vascular permeability was examined on day 9 of infection in selected tissues from treated mice to assess the impact of MY-24. Serum EBD content was reduced in the TCRV-infected animals on day 9, suggesting vascular hyperpermeability (Figure 13A). In liver, kidney, and spleen, higher average of tissue to serum EBD ratio was observed in the TCRV-infected animals compared to the normal sham-infected mice (Figure 13B, C, E). In general, the tissue EDB ratios were lower in the MY-24 treated mice compared to placebo-treated animals, suggesting that MY-24 may be reducing vascular leakage.

www.manaraa.com

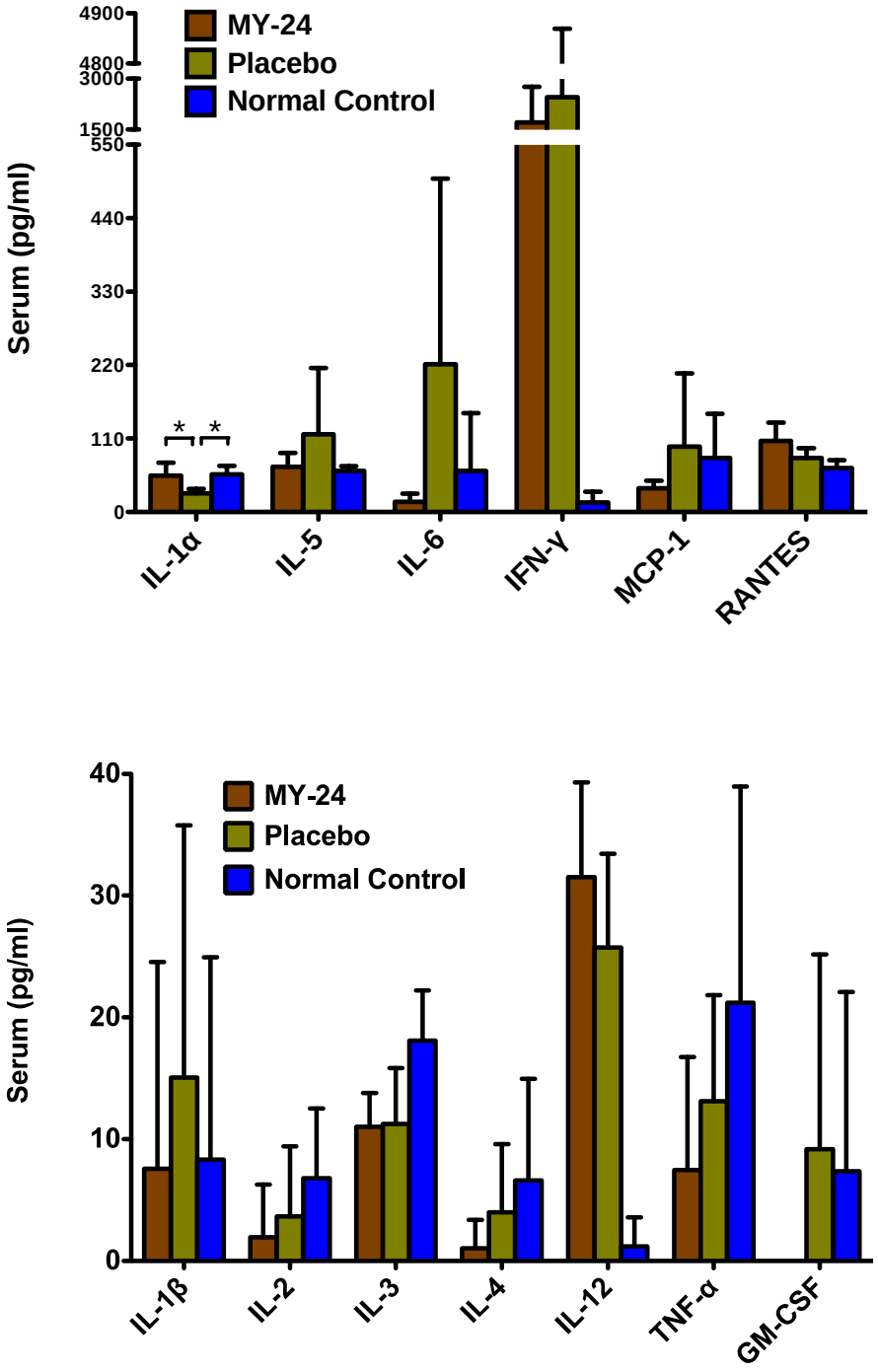

Figure 11. Comparative Analysis of Serum Cytokine Levels in Mice Infected with TCRV and Treated with MY-24 or Placebo. As described in Figure 8, TCRV-infected animals treated with MY-24 (n=5) or placebo (n=5) were sacrificed on day 8 relative to the time of infection. Shown are the serum concentrations of selected cytokines determined using a multiplexed array. *$P < 0.05$.

www.manaraa.com

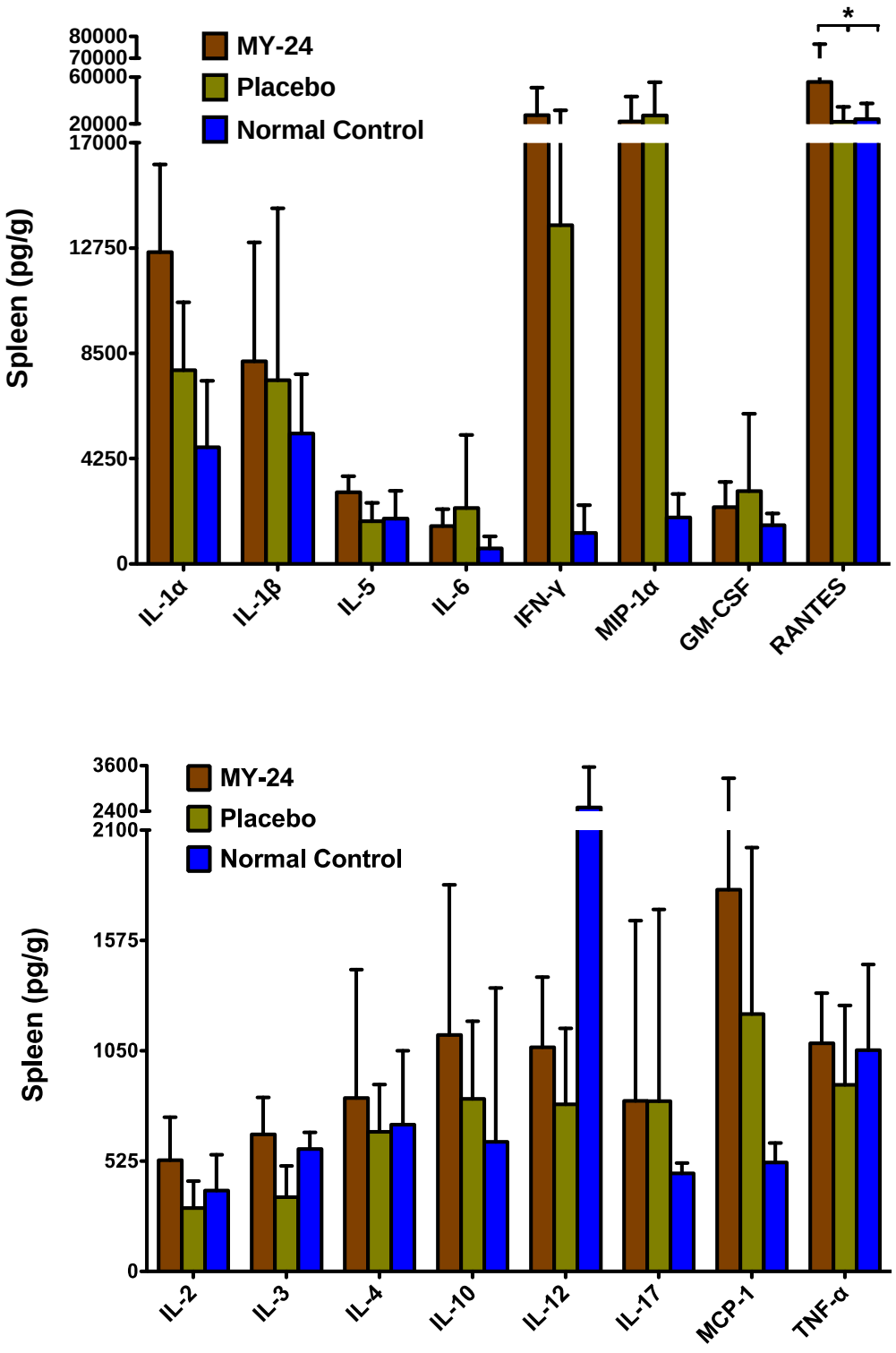

Figure 12. Comparative Analysis of Spleen Cytokine Levels in Mice Infected with TCRV and Treated with MY-24 or Placebo. As described in Figure 8, TCRV-infected animals treated with MY-24 (n=5) or placebo (n=5) were sacrificed on day 8 relative to the time of infection. Shown are the splenic concentrations of selected cytokines determined using a multiplexed array. *$P < 0.05$.

www.manaraa.com

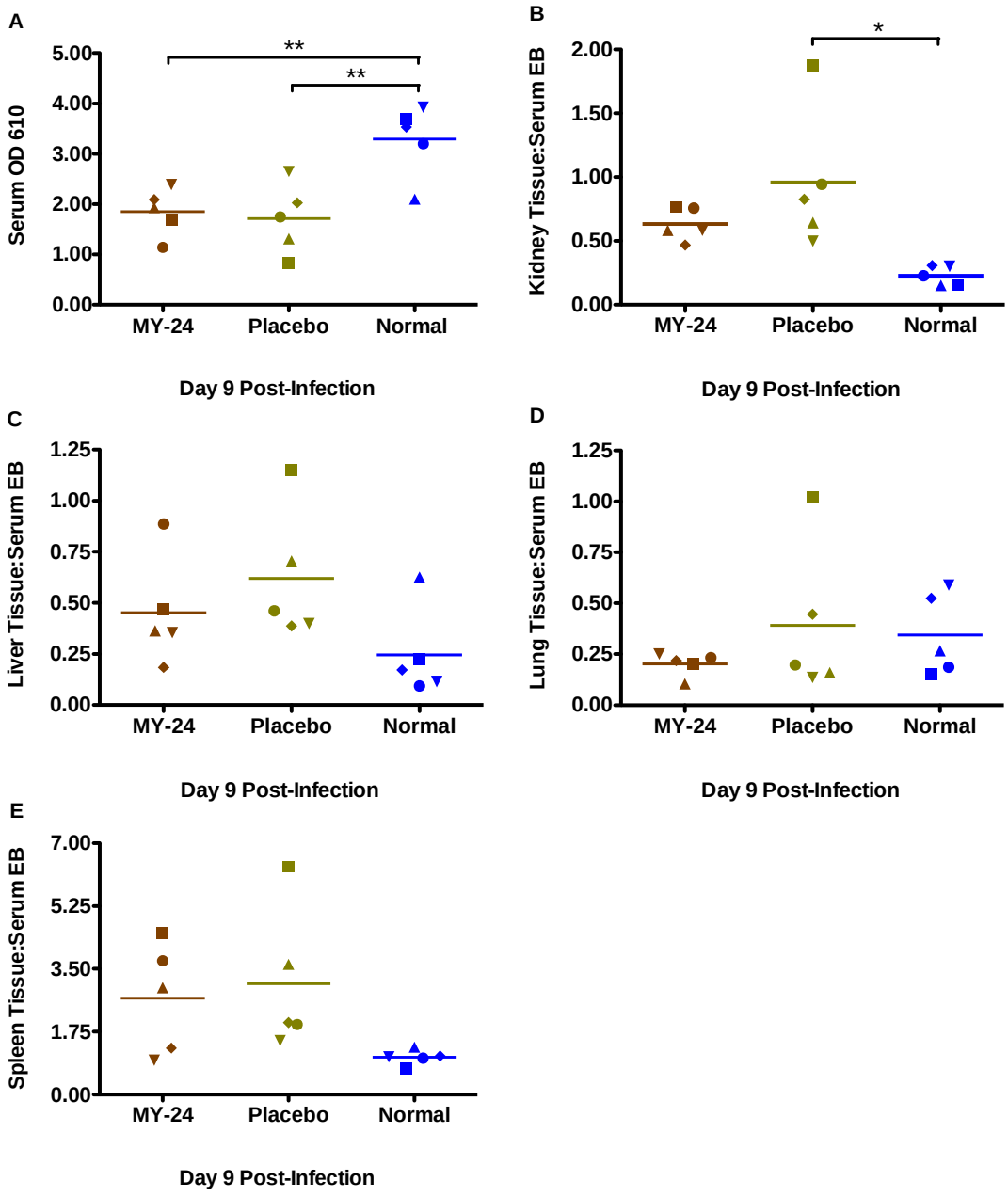

Figure 13. Evaluation of Vascular Permeability in TCRV-Infected Mice Treated with MY-24. TCRV-infected mice treated with MY-24 or placebo, starting 3 days after challenge, were infused with EB dye on day 9 of infection and systemic levels, as well as leakage into the viscera was evaluated. A) Serum EB dye levels and ratios of tissue to respective serum levels are shown for B) liver, C) kidney, D) lung, and E) spleen tissues. *$P < 0.05$, ** $P < 0.01$ compared to sham-infected animals.

www.manaraa.com

However, the effect was slight in most cases, and the differences were not statistically significant (Figure 13B-E).

www.manaraa.com

CHAPTER 4

DISCUSSION

Junin and other South American hemorrhagic fever-causing arenaviruses pose a considerable public health threat as emerging infectious disease agents and because of their potential for intentional release. Further research to better understand the HF disease process to aid the development of therapeutic and prophylactic interventions is needed; however, all of the highly pathogenic NWA (Junin, Machupo, Guanarito, Sabia), including the recently identified Chapare virus, require BSL-4 containment facilities for their study. TCRV is a nonpathogenic NWA that is closely related to JUNV at the amino acid level [7]. Due to the high cost and relative inaccessibility of BSL-4 facilities, TCRV, which can be worked with in BSL-2 containment, facilitates early stage preclinical development of promising antiviral compounds. However, despite its relatedness to the highly pathogenic NWA, TCRV lacks the ability to antagonize the host IFN response [88], and therefore requires AG129 IFN receptor-deficient mice as hosts for productive infection. We employed the TCRV AG129 infection model to test the hypothesis that MY-24 protects AG129 mice from lethal TCRV infection by subduing the inflammatory response and limiting vascular leak.

The initial objective of this study was to characterize the natural history of disease for the AG129 mouse TCRV infection model to compare the disease to the human condition and determine the optimal time to evaluate the effects of MY-24 on the disease process. The first part involved determining the kinetics of viral replication in blood and tissues, assessing changes in clinical and hematologic parameters, tracking histopathological changes, and cytokine profiling during the course of infection. The

www.manaraa.com

second part of the initial objective was to determine if and when TCRV infection increased vascular permeability characteristic of viral HF syndromes. The careful characterization of the model paved the way for studies to evaluate the effects of MY-24 on the host response to infection. The hypothesis suggesting that MY-24 is primarily acting by dampening an overzealous inflammatory response was borne out of the findings from the original work that reported robust protection afforded by MY-24 treatment without any reduction in viral burden [76]. The results from the present study confirm the previous finding; however, there was a trend suggesting that MY-24 may be having a slight effect in reducing titers in serum and some tissues. Nevertheless, the lack of statistically significant reductions in viral loads argues against a direct antiviral effect.

The current paradigm in the viral HF field is that exaggerated release of proinflammatory cytokines into the circulation is the cause of the devastating vascular leakage that leads to systemic shock, multi-organ failure, and death [101,109]. With this in mind, the treatment of advanced cases of viral HF would likely require a combination of an effective antiviral that directly disrupts the virus life cycle with an agent that can limit the collateral damage caused by an overly aggressive host response. Our data measuring vascular integrity in mice during the acute phase of TCRV infection indicates that vascular leak is a part of the disease process, but its overall contribution to the decline of the animals is difficult to measure.

In general, our collective natural history data are consistent with the idea that increasing viral burden in the blood leads to release of proinflammatory cytokines that drive vascular leak, which likely contributes to the demise of the animals. Indeed, low-level viremia begins on day 6 post infection (Figure 1), at which time elevations in

www.manaraa.com

systemic proinflammatory mediators such as IL-6, MCP-1, and TNF-α are detected (Figure 4), and likely contribute to the increased vascular permeability which begins on day 8 (Figure 7), and may contribute to mortality commonly observed between days 9-11. IL-6, which has been associated with severe disease in cases of viral HF and bacterial sepsis [110,111], was slightly reduced on day 8 of infection in mice treated with MY-24. This, in addition to slight reductions in the levels of MCP-1 and TNF-α, may be sufficient to alter the disease course in a way that MY-24-treated animals are able to survive the infection.

We predicted that a reduction in certain key inflammatory cytokines by MY-24 treatment would lead to diminished vascular leak. Although there was a trend of lower accumulation of EBD in tissues of mice receiving MY-24, the differences were not significant when measured on day 9 post infection (Figure 13). Because we only assayed for vascular permeability on day 9, it is conceivable that MY-24 could have reduced the duration of the vascular leak or delayed its onset. Such changes in the kinetics of vascular leak could make a difference between life and death.

A modified version of our hypothesis is that MY-24 simply delays the deleterious hyperimmune response, thereby changing the dynamics of the disease and the onset and degree of vascular leak in a way that produces a more manageable disease. Our MY-24 cytokine profiling data are consistent with this idea (Figures 11, 12). Moreover, neutralizing antibody responses appeared to be delayed in the MY-24 treated mice compared to animals receiving placebo (Figure 10). Notably, surviving animals treated with MY-24 appear ill (ruffled fur, lethargy, weight loss) during the second and third weeks of the infection, compared to the mice treated with placebo which generally show

www.manaraa.com

clinical signs a day or two earlier. If too vigorous of a host response is largely responsible for TCRV-induced disease, the ability of MY-24 to slow the process may be sufficient to prevent mortality and allow the adaptive immune response to help control the systemic infection, as suggested by the PRNT data and the eventual clearance of the virus from the circulation.

As reported in our initial publication describing the TCRV model [76], the spleen was the first site where significant viral loads were detected, and only it and liver tissue presented with it considerable histopathology. Unexpectedly, we found >9.5 logs of virus in the spleens of 3 of 5 mice treated with MY-24, approximately 3 logs greater than the observed titers for the other two mice and the 5 animals that were treated with placebo (Figure 9D). In fact, the spleen was the only tissue in which there was more virus present compared to the placebo group, and this was also observed, but to a lesser degree, in the previously reported study [76]. The effects of the increased viral load were reflected in higher cytokine levels in day 8 spleen homogenates from MY-24-treated mice. The importance of this finding and how it may contribute to the survival of mice treated with MY-24 is unclear.

In regards to the immune response to TCRV in the AG129 mice, we were surprised to see a general reduction in kidney and brain tissue cytokine levels (Figure 4). Although virus did appear later in these tissues, we would not of predicted the overall suppressive effect observed. The subdued proinflammatory cytokine response in kidney and brain tissues presumably accounts for the lack of pathology. The more robust cytokine responses in spleen, liver, and lung tissues were consistent with the more prominent pathology observed in those tissues, and suggest immunopathology. Interestingly, the

www.manaraa.com

brain was the only tissue in which viral loads increased gradually out to 32 days post infection (Figure 8E). This is striking in that systemic virus was cleared by day 24 (Figure 8A). This suggests that the high and constant titers found in the brains of TCRV-challenged animals on days 24, 32, and 40 were the results of viral replication and persistence in the brain, and not continued seeding from circulating virus.

Arenaviruses are zoonotic agents that produce subclinical infections in their respective rodent reservoir species. An interesting and unexpected finding from our studies was that surviving mice go on to develop chronic infection in various tissues, despite clearing the virus systemically. We found that the weight loss nadir in MY-24-treated mice from days 18 to 21, prior to the recovery of the animals, is consistent with the systemic clearance of the virus between the 16 and 24 day time points. Importantly, however, the AG129 mice lack type I and II IFN receptors, and thus it is difficult to make conclusions regarding the biological significance of this finding. Notwithstanding, it is likely that arenaviruses antagonize native rodent IFN response pathways as a mechanism by which they establish chronic carrier states. Additional studies investigating the long-term carriage of TCRV in AG129 mice may lead to new insights in arenavirus-rodent reservoir interactions.

Taken together, our data provides evidence that an increase in systemic TCRV levels is followed by hypercytokinemia, which likely drives the observed vascular leak in the AG129 mouse model. Ensuing plasma volume loss, organ failure, and shock are believed to be the cause of death. In MY-24-treated mice there was an overall slight reduction in serum viral load, a slight decrease in IL-6, IFN-γ and MCP-1 (with a minimal reduction in other proinflammatory cytokines) (Figure 11), and a trend of

www.manaraa.com

reduced vascular permeability in several tissues (Figure 13). We expected a more dramatic effect for MY-24 treatment in reducing inflammatory responses and improving vascular integrity, which was the basis of our hypothesis. However, it is possible that even a slight effect in the measured parameters could be sufficient to alter the outcome of TCRV infection. Certainly, there are other factors that contribute to the fatal outcome of TCRV infection in AG129 mice, and MY-24 may be having a more substantial effect in that context. What appears to be clear is that despite having activity against TCRV *in vitro*, there is little evidence for a direct antiviral effect targeting the virus life cycle *in vivo*. Our continued line of thinking is that MY-24 is blunting several response pathways in the AG129 host response sufficient to alter the outcome of TCRV infection.

www.manaraa.com

REFERENCES

1. Nunberg JH, York J (2012) The curious case of arenavirus entry, and its inhibition. Viruses 4: 83-101.

2. Bowen MD, Peters CJ, Nichol ST (1996) The phylogeny of New World (Tacaribe complex) arenaviruses. Virology 219: 285-290.

3. Wolff H, Lange JV, Webb PA (1978) Interrelationships among arenaviruses measured by indirect immunofluorescence. Intervirology 9: 344-350.

4. Bowen MD, Peters CJ, Nichol ST (1997) Phylogenetic analysis of the Arenaviridae: Patterns of virus evolution and evidence for cospeciation between arenaviruses and their rodent hosts. Mol Phylogenet Evol 8: 301-316.

5. Paweska JT, Sewlall NH, Ksiazek TG, Blumberg LH, Hale MJ, et al. (2009) Nosocomial outbreak of novel arenavirus infection, southern Africa. Emerg Infect Dis 15: 1598-1602.

6. Moraz ML, Kunz S (2011) Pathogenesis of arenavirus hemorrhagic fevers. Expert Rev Anti Infect Ther 9: 49-59.

7. Briese T, Paweska JT, McMullan LK, Hutchison SK, Street C, et al. (2009) Genetic detection and characterization of Lujo virus, a new hemorrhagic fever-associated arenavirus from southern Africa. PLoS Pathog 5: e1000455.

8. Gowen BB, Bray M (2011) Progress in the experimental therapy of severe arenaviral infections. Future Microbiol 6: 1429-1441.

9. Downs WG, Anderson CR, Spence L, Aitken TH, Greenhall AH (1963) Tacaribe virus, a new agent isolated from Artibeus bats and mosquitoes in Trinidad, West Indies. Am J Trop Med Hyg 12: 640-646.

10. Enria DA, Briggiler AM, Sanchez Z (2008) Treatment of Argentine hemorrhagic fever. Antiviral Res 78: 132-139.

11. Rodrigo WW, Ortiz-Riano E, Pythoud C, Kunz S, de la Torre JC, et al. (2012) Arenavirus nucleoproteins prevent activation of nuclear factor kappa B. J Virol 86: 8185-8197.

12. Borio L, Inglesby T, Peters CJ, Schmaljohn AL, Hughes JM, et al. (2002) Hemorrhagic fever viruses as biological weapons: Medical and public health management. JAMA 287: 2391-2405.

www.manaraa.com

13. Enria DA, Ambrosio AM, Briggiler AM, Feuillade MR, Crivelli E (2010) Candid#1 vaccine against Argentine hemorrhagic fever produced in Argentina. Immunogenicity and safety. Medicina (B Aires) 70: 215-222.

14. Mills JN, Ellis BA, Childs JE, McKee KT, Jr., Maiztegui JI, et al. (1994) Prevalence of infection with Junin virus in rodent populations in the epidemic area of Argentine hemorrhagic fever. Am J Trop Med Hyg 51: 554-562.

15. Young PR, Howard CR (1983) Fine structure analysis of Pichinde virus nucleocapsids. J Gen Virol 64 (Pt 4): 833-842.

16. Bonthius DJ, Wright R, Tseng B, Barton L, Marco E, et al. (2007) Congenital lymphocytic choriomeningitis virus infection: Spectrum of disease. Ann Neurol 62: 347-355.

17. Fischer SA, Graham MB, Kuehnert MJ, Kotton CN, Srinivasan A, et al. (2006) Transmission of lymphocytic choriomeningitis virus by organ transplantation. N Engl J Med 354: 2235-2249.

18. Buckley SM, Casals J (1970) Lassa fever, a new virus disease of man from West Africa. 3. Isolation and characterization of the virus. Am J Trop Med Hyg 19: 680-691.

19. Ogbu O, Ajuluchukwu E, Uneke CJ (2007) Lassa fever in West African sub-region: An overview. J Vector Borne Dis 44: 1-11.

20. Fisher-Hoch SP, Tomori O, Nasidi A, Perez-Oronoz GI, Fakile Y, et al. (1995) Review of cases of nosocomial Lassa fever in Nigeria: The high price of poor medical practice. BMJ 311: 857-859.

21. McCormick JB, King IJ, Webb PA, Johnson KM, O'Sullivan R, et al. (1987) A case-control study of the clinical diagnosis and course of Lassa fever. J Infect Dis 155: 445-455.

22. McCormick JB, King IJ, Webb PA, Scribner CL, Craven RB, et al. (1986) Lassa fever. Effective therapy with ribavirin. New England Journal of Medicine 314: 20-26.

23. Khan SH, Goba A, Chu M, Roth C, Healing T, et al. (2008) New opportunities for field research on the pathogenesis and treatment of Lassa fever. Antiviral Res 78: 103-115.

24. Bausch DG, Hadi CM, Khan SH, Lertora JJ (2010) Review of the literature and proposed guidelines for the use of oral ribavirin as postexposure prophylaxis for Lassa fever. Clin Infect Dis 51: 1435-1441.

www.manaraa.com

25. Rowe WP, Murphy FA, Bergold GH, Casals J, Hotchin J, et al. (1970) Arenoviruses: Proposed name for a newly defined virus group. J Virol 5: 651-652.

26. Auperin DD, Romanowski V, Galinski M, Bishop DH (1984) Sequencing studies of pichinde arenavirus S RNA indicate a novel coding strategy, an ambisense viral S RNA. J Virol 52: 897-904.

27. Lenz O, ter Meulen J, Klenk HD, Seidah NG, Garten W (2001) The Lassa virus glycoprotein precursor GP-C is proteolytically processed by subtilase SKI-1/S1P. Proc Natl Acad Sci U S A 98: 12701-12705.

28. Harnish DG, Dimock K, Bishop DH, Rawls WE (1983) Gene mapping in Pichinde virus: Assignment of viral polypeptides to genomic L and S RNAs. J Virol 46: 638-641.

29. Urata S, de la Torre JC (2011) Arenavirus budding. Adv Virol 2011: 180326.

30. Salvato MS, Schweighofer KJ, Burns J, Shimomaye EM (1992) Biochemical and immunological evidence that the 11 kDa zinc-binding protein of lymphocytic choriomeningitis virus is a structural component of the virus. Virus Res 22: 185-198.

31. Lopez N, Jacamo R, Franze-Fernandez MT (2001) Transcription and RNA replication of tacaribe virus genome and antigenome analogs require N and L proteins: Z protein is an inhibitor of these processes. J Virol 75: 12241-12251.

32. Salvato M, Shimomaye E, Oldstone MB (1989) The primary structure of the lymphocytic choriomeningitis virus L gene encodes a putative RNA polymerase. Virology 169: 377-384.

33. Beyer WR, Popplau D, Garten W, von Laer D, Lenz O (2003) Endoproteolytic processing of the lymphocytic choriomeningitis virus glycoprotein by the subtilase SKI-1/S1P. J Virol 77: 2866-2872.

34. Vezza AC, Gard GP, Compans RW, Bishop DH (1977) Structural components of the arenavirus Pichinde. J Virol 23: 776-786.

35. Radoshitzky SR, Kuhn JH, Spiropoulou CF, Albarino CG, Nguyen DP, et al. (2008) Receptor determinants of zoonotic transmission of New World hemorrhagic fever arenaviruses. Proc Natl Acad Sci U S A 105: 2664-2669.

36. Radoshitzky SR, Abraham J, Spiropoulou CF, Kuhn JH, Nguyen D, et al. (2007) Transferrin receptor 1 is a cellular receptor for New World haemorrhagic fever arenaviruses. Nature 446: 92-96.

www.manaraa.com

37. Abraham J, Kwong JA, Albarino CG, Lu JG, Radoshitzky SR, et al. (2009) Host-species transferrin receptor 1 orthologs are cellular receptors for nonpathogenic new world clade B arenaviruses. PLoS Pathog 5: e1000358.

38. Cao W, Henry MD, Borrow P, Yamada H, Elder JH, et al. (1998) Identification of alpha-dystroglycan as a receptor for lymphocytic choriomeningitis virus and Lassa fever virus. Science 282: 2079-2081.

39. Rojek JM, Spiropoulou CF, Kunz S (2006) Characterization of the cellular receptors for the South American hemorrhagic fever viruses Junin, Guanarito, and Machupo. Virology 349: 476-491.

40. Pasqual G, Rojek JM, Masin M, Chatton JY, Kunz S (2011) Old world arenaviruses enter the host cell via the multivesicular body and depend on the endosomal sorting complex required for transport. PLoS Pathog 7: e1002232.

41. Pinschewer DD, Perez M, de la Torre JC (2003) Role of the virus nucleoprotein in the regulation of lymphocytic choriomeningitis virus transcription and RNA replication. J Virol 77: 3882-3887.

42. Cornu TI, de la Torre JC (2001) RING finger Z protein of lymphocytic choriomeningitis virus (LCMV) inhibits transcription and RNA replication of an LCMV S-segment minigenome. J Virol 75: 9415-9426.

43. Lee KJ, Novella IS, Teng MN, Oldstone MB, de La Torre JC (2000) NP and L proteins of lymphocytic choriomeningitis virus (LCMV) are sufficient for efficient transcription and replication of LCMV genomic RNA analogs. J Virol 74: 3470-3477.

44. Perez M, Craven RC, de la Torre JC (2003) The small RING finger protein Z drives arenavirus budding: Implications for antiviral strategies. Proc Natl Acad Sci U S A 100: 12978-12983.

45. Borrow P, Martinez-Sobrido L, de la Torre JC (2010) Inhibition of the type I interferon antiviral response during arenavirus infection. Viruses 2: 2443-2480.

46. Fan L, Briese T, Lipkin WI (2010) Z proteins of New World arenaviruses bind RIG-I and interfere with type I interferon induction. J Virol 84: 1785-1791.

47. Stephen EL, Jahrling PB (1979) Experimental Lassa fever virus infection successfully treated with ribavirin. Lancet 1: 268-269.

48. Kiley MP, Lange JV, Johnson KM (1979) Protection of rhesus monkeys from Lassa virus by immunisation with closely related Arenavirus. Lancet 2: 738.

www.manaraa.com

49. Jahrling PB, Hesse RA, Eddy GA, Johnson KM, Callis RT, et al. (1980) Lassa virus infection of rhesus monkeys: Pathogenesis and treatment with ribavirin. J Infect Dis 141: 580-589.

50. Stephenson EH, Larson EW, Dominik JW (1984) Effect of environmental factors on aerosol-induced Lassa virus infection. J Med Virol 14: 295-303.

51. Jahrling PB, Peters CJ, Stephen EL (1984) Enhanced treatment of Lassa fever by immune plasma combined with ribavirin in cynomolgus monkeys. J Infect Dis 149: 420-427.

52. Hensley LE, Smith MA, Geisbert JB, Fritz EA, Daddario-DiCaprio KM, et al. (2011) Pathogenesis of Lassa fever in cynomolgus macaques. Virol J 8: 205.

53. Carrion R, Jr., Brasky K, Mansfield K, Johnson C, Gonzales M, et al. (2007) Lassa virus infection in experimentally infected marmosets: Liver pathology and immunophenotypic alterations in target tissues. J Virol 81: 6482-6490.

54. Walker DH, Wulff H, Lange JV, Murphy FA (1975) Comparative pathology of Lassa virus infection in monkeys, guinea-pigs, and Mastomys natalensis. Bull World Health Organ 52: 523-534.

55. Jahrling PB, Smith S, Hesse RA, Rhoderick JB (1982) Pathogenesis of Lassa virus infection in guinea pigs. Infect Immun 37: 771-778.

56. Flatz L, Rieger T, Merkler D, Bergthaler A, Regen T, et al. (2010) T cell-dependence of Lassa fever pathogenesis. PLoS Pathog 6: e1000836.

57. Bird BH, Dodd KA, Erickson BR, Albarino CG, Chakrabarti AK, et al. (2012) Severe hemorrhagic Fever in strain 13/n Guinea pigs infected with lujo virus. PLoS Negl Trop Dis 6: e1801.

58. Lukashevich IS, Djavani M, Rodas JD, Zapata JC, Usborne A, et al. (2002) Hemorrhagic fever occurs after intravenous, but not after intragastric, inoculation of rhesus macaques with lymphocytic choriomeningitis virus. J Med Virol 67: 171-186.

59. Buchmeier MJ, Welsh RM, Dutko FJ, Oldstone MB (1980) The virology and immunobiology of lymphocytic choriomeningitis virus infection. Adv Immunol 30: 275-331.

60. Jahrling PB, Hesse RA, Rhoderick JB, Elwell MA, Moe JB (1981) Pathogenesis of a pichinde virus strain adapted to produce lethal infections in guinea pigs. Infect Immun 32: 872-880.

www.manaraa.com

61. Connolly BM, Jenson AB, Peters CJ, Geyer SJ, Barth JF, et al. (1993) Pathogenesis of Pichinde virus infection in strain 13 guinea pigs: an immunocytochemical, virologic, and clinical chemistry study. Am J Trop Med Hyg 49: 10-24.

62. Aronson JF, Herzog NK, Jerrells TR (1994) Pathological and virological features of arenavirus disease in guinea pigs. Comparison of two Pichinde virus strains. Am J Pathol 145: 228-235.

63. Buchmeier MJ, Rawls WE (1977) Variation between strains of hamsters in the lethality of Pichinde virus infections. Infect Immun 16: 413-421.

64. Murphy FA, Buchmeier MJ, Rawls WE (1977) The reticuloendothelium as the target in a virus infection. Pichinde virus pathogenesis in two strains of hamsters. Lab Invest 37: 502-515.

65. Gowen BB, Julander JG, London NR, Wong MH, Larson D, et al. (2010) Assessing changes in vascular permeability in a hamster model of viral hemorrhagic fever. Virol J 7: 240.

66. Xiao SY, Zhang H, Yang Y, Tesh RB (2001) Pirital virus (Arenaviridae) infection in the syrian golden hamster, Mesocricetus auratus: A new animal model for arenaviral hemorrhagic fever. Am J Trop Med Hyg 64: 111-118.

67. Sbrana E, Mateo RI, Xiao SY, Popov VL, Newman PC, et al. (2006) Clinical laboratory, virologic, and pathologic changes in hamsters experimentally infected with Pirital virus (Arenaviridae): a rodent model of Lassa fever. Am J Trop Med Hyg 74: 1096-1102.

68. McKee KT, Jr., Mahlandt BG, Maiztegui JI, Green DE, Peters CJ (1987) Virus-specific factors in experimental Argentine hemorrhagic fever in rhesus macaques. J Med Virol 22: 99-111.

69. Green DE, Mahlandt BG, McKee KT, Jr. (1987) Experimental Argentine hemorrhagic fever in rhesus macaques: Virus-specific variations in pathology. J Med Virol 22: 113-133.

70. Weissenbacher MC, Calello MA, Colillas OJ, Rondinone SN, Frigerio MJ (1979) Argentine hemorrhagic fever: A primate model. Intervirology 11: 363-365.

71. Gonzalez PH, Laguens RP, Frigerio MJ, Calello MA, Weissenbacher MC (1983) Junin virus infection of Callithrix jacchus: Pathologic features. Am J Trop Med Hyg 32: 417-423.

www.manaraa.com

72. Molinas FC, Paz RA, Rimoldi MT, de Bracco MM (1978) Studies of blood coagulation and pathology in experimental infection of guinea pigs with Junin virus. J Infect Dis 137: 740-746.

73. Oubina JR, Carballal G, Videla CM, Cossio PM (1984) The guinea pig model for Argentine hemorrhagic fever. Am J Trop Med Hyg 33: 1251-1257.

74. Yun NE, Linde NS, Dziuba N, Zacks MA, Smith JN, et al. (2008) Pathogenesis of XJ and Romero strains of Junin virus in two strains of guinea pigs. Am J Trop Med Hyg 79: 275-282.

75. Kolokoltsova OA, Yun NE, Poussard AL, Smith JK, Smith JN, et al. (2010) Mice lacking alpha/beta and gamma interferon receptors are susceptible to junin virus infection. J Virol 84: 13063-13067.

76. Gowen BB, Wong MH, Larson D, Ye W, Jung KH, et al. (2010) Development of a new tacaribe arenavirus infection model and its use to explore antiviral activity of a novel aristeromycin analog. PLoS One 5.

77. Terrell TG, Stookey JL, Eddy GA, Kastello MD (1973) Pathology of Bolivian hemorrhagic fever in the rhesus monkey. Am J Pathol 73: 477-494.

78. Eddy GA, Scott SK, Wagner FS, Brand OM (1975) Pathogenesis of Machupo virus infection in primates. Bull World Health Organ 52: 517-521.

79. Kastello MD, Eddy GA, Kuehne RW (1976) A rhesus monkey model for the study of Bolivian hemorrhagic fever. J Infect Dis 133: 57-62.

80. Wagner FS, Eddy GA, Brand OM (1977) The African green monkey as an alternate primate host for studying Machupo virus infection. Am J Trop Med Hyg 26: 159-162.

81. McLeod CG, Jr., Stookey JL, White JD, Eddy GA, Fry GA (1978) Pathology of Bolivian hemorrhagic fever in the African green monkey. Am J Trop Med Hyg 27: 822-826.

82. Webb PA, Justines G, Johnson KM (1975) Infection of wild and laboratory animals with Machupo and Latino viruses. Bull World Health Organ 52: 493-499.

83. Bradfute SB, Stuthman KS, Shurtleff AC, Bavari S (2011) A STAT-1 knockout mouse model for Machupo virus pathogenesis. Virol J 8: 300.

84. Hall WC, Geisbert TW, Huggins JW, Jahrling PB (1996) Experimental infection of guinea pigs with Venezuelan hemorrhagic fever virus (Guanarito): A model of human disease. Am J Trop Med Hyg 55: 81-88.

www.manaraa.com

85. Carlton M, Gillespie, R., Garver, J., Graguljic, D., Vela, E.M. (2012) The Syrian Golden Hamster as a Model to Study Flexal Virus Pathogenesis. iMedPub, Internet Medical Publishing, Mar 29, 2012.

86. Bolken TC, Laquerre S, Zhang Y, Bailey TR, Pevear DC, et al. (2006) Identification and characterization of potent small molecule inhibitor of hemorrhagic fever New World arenaviruses. Antiviral Res 69: 86-97.

87. Grajkowski A, Pedras-Vasconcelos J, Wang V, Ausin C, Hess S, et al. (2005) Thermolytic CpG-containing DNA oligonucleotides as potential immunotherapeutic prodrugs. Nucleic Acids Res 33: 3550-3560.

88. Martinez-Sobrido L, Giannakas P, Cubitt B, Garcia-Sastre A, de la Torre JC (2007) Differential inhibition of type I interferon induction by arenavirus nucleoproteins. J Virol 81: 12696-12703.

89. Cashman KA, Smith MA, Twenhafel NA, Larson RA, Jones KF, et al. (2011) Evaluation of Lassa antiviral compound ST-193 in a guinea pig model. Antiviral Res 90: 70-79.

90. Thomas CJ, Casquilho-Gray HE, York J, DeCamp DL, Dai D, et al. (2011) A specific interaction of small molecule entry inhibitors with the envelope glycoprotein complex of the Junin hemorrhagic fever arenavirus. J Biol Chem 286: 6192-6200.

91. York J, Dai D, Amberg SM, Nunberg JH (2008) pH-induced activation of arenavirus membrane fusion is antagonized by small-molecule inhibitors. J Virol 82: 10932-10939.

92. Leyssen P, De Clercq E, Neyts J (2008) Molecular strategies to inhibit the replication of RNA viruses. Antiviral Res 78: 9-25.

93. Furuta Y, Takahashi K, Fukuda Y, Kuno M, Kamiyama T, et al. (2002) In vitro and in vivo activities of anti-influenza virus compound T-705. Antimicrob Agents Chemother 46: 977-981.

94. Takahashi K, Furuta Y, Fukuda Y, Kuno M, Kamiyama T, et al. (2003) In vitro and in vivo activities of T-705 and oseltamivir against influenza virus. Antivir Chem Chemother 14: 235-241.

95. Furuta Y, Takahashi K, Shiraki K, Sakamoto K, Smee DF, et al. (2009) T-705 (favipiravir) and related compounds: Novel broad-spectrum inhibitors of RNA viral infections. Antiviral Res 82: 95-102.

www.manaraa.com

96. Mendenhall M, Russell A, Juelich T, Messina EL, Smee DF, et al. (2011) T-705 (favipiravir) inhibition of arenavirus replication in cell culture. Antimicrob Agents Chemother 55: 782-787.

97. Furuta Y, Takahashi K, Kuno-Maekawa M, Sangawa H, Uehara S, et al. (2005) Mechanism of action of T-705 against influenza virus. Antimicrob Agents Chemother 49: 981-986.

98. Gowen BB, Smee DF, Wong MH, Hall JO, Jung KH, et al. (2008) Treatment of late stage disease in a model of arenaviral hemorrhagic fever: T-705 efficacy and reduced toxicity suggests an alternative to ribavirin. PLoS One 3: e3725.

99. Mendenhall M, Russell A, Smee DF, Hall JO, Skirpstunas R, et al. (2011) Effective oral favipiravir (T-705) therapy initiated after the onset of clinical disease in a model of arenavirus hemorrhagic Fever. PLoS Negl Trop Dis 5: e1342.

100. Bray M (2005) Pathogenesis of viral hemorrhagic fever. Curr Opin Immunol 17: 399-403.

101. Geisbert TW, Jahrling PB (2004) Exotic emerging viral diseases: Progress and challenges. Nat Med 10: S110-121.

102. Schneller SW (2002) Carbocyclic nucleosides (carbanucleosides) as new therapeutic leads. Curr Top Med Chem 2: 1087-1092.

103. Yang M, Schneller SW (2005) 5'-Homoaristeromycin. Synthesis and antiviral activity against orthopox viruses. Bioorg Med Chem Lett 15: 149-151.

104. Borchardt RT (1980) S-Adenosyl-L-methionine-dependent macromolecule methyltransferases: Potential targets for the design of chemotherapeutic agents. J Med Chem 23: 347-357.

105. Bennett LL, Jr., Allan PW, Rose LM, Comber RN, Secrist JA, 3rd (1986) Differences in the metabolism and metabolic effects of the carbocyclic adenosine analogs, neplanocin A and aristeromycin. Mol Pharmacol 29: 383-390.

106. Bennett LL, Jr., Bowdon BJ, Allan PW, Rose LM (1986) Evidence that the carbocyclic analog of adenosine has different mechanisms of cytotoxicity to cells with adenosine kinase activity and to cells lacking this enzyme. Biochem Pharmacol 35: 4106-4109.

107. Yang M, Ye W, Schneller SW (2004) Preparation of carbocyclic S-adenosylazamethionine accompanied by a practical synthesis of (-)-aristeromycin. J Org Chem 69: 3993-3996.

www.manaraa.com

108. Carballal G, Cossio PM, Oubina JR, de la Vega MT, Nagle C, et al. (1983) Experimental infection of a South American primate, the Cebus sp, with XJ strain of Junin virus. Medicina (B Aires) 43: 639-646.

109. Bray GA (2005) Epidemiology, risks and pathogenesis of obesity. Meat Sci 71: 2-7.

110. Calandra T, Gerain J, Heumann D, Baumgartner JD, Glauser MP (1991) High circulating levels of interleukin-6 in patients with septic shock: Evolution during sepsis, prognostic value, and interplay with other cytokines. The Swiss-Dutch J5 Immunoglobulin Study Group. Am J Med 91: 23-29.

111. Damas P, Ledoux D, Nys M, Vrindts Y, De Groote D, et al. (1992) Cytokine serum level during severe sepsis in human IL-6 as a marker of severity. Ann Surg 215: 356-362.

www.manaraa.com

APPENDIX

www.manaraa.com

Table A1. Summary of Histopathology Findings from Mice Infected with TCRV

Mouse no.	Liver	Spleen	Lung	Kidney	Brain	Day Post Infection
211		Hyperplastic splenic follicles with increased numbers of neutrophils				7
212		Hyperplastic splenic follicles				7
228		Hyperplastic splenic follicles with increased numbers of neutrophils				7
229		Hyperplastic splenic follicles				7
213	Moderate numbers of lymphocytes and histiocytes infiltrate portal zones Widely scattered individual hepatocytes are degenerate/necrotic and are surrounded by small numbers of neutrophils or lymphocytes.	Hyperplastic splenic follicles with scattered lytic cells	Mild perivascular edema with small numbers of mixed inflammatory cells or moderate perivascular hemorrhage surrounding scattered pulmonary arterioles.			8
214	"Moderate numbers of lymphocytes and histiocytes infiltrate portal zones Widely scattered individual hepatocytes are degenerate/necrotic and are surrounded by small numbers of neutrophils or lymphocytes."	Hyperplastic splenic follicles with scattered lytic cells and increased numbers of neutrophils.				8
230	Moderate numbers of lymphocytes and histiocytes infiltrate portal zones (liver). Widely scattered individual hepatocytes are necrotic and are surrounded by small numbers of neutrophils or lymphocytes.	Hyperplastic splenic follicles with scattered lytic cells				8

www.manaraa.com

Mouse no.	Liver	Spleen	Lung	Kidney	Brain	Day Post Infection
246	Moderate numbers of lymphocytes and histiocytes infiltrate portal zones (liver). Scattered individual hepatocytes are degenerate/necrotic and are surrounded by small numbers of neutrophils or lymphocytes.	Hyperplastic splenic follicles with increased numbers of neutrophils.				8
215	Moderate numbers of lymphocytes, neutrophils and histiocytes infiltrate portal zones and accumulate in sinusoidal spaces. Scattered individual hepatocytes are degenerate/necrotic and are surrounded by aggregates of neutrophils and lymphocytes.	Hyperplastic splenic follicles with scattered lytic cells.	Perivascular edema fluid with small numbers of neutrophils or perivascular hemorrhage surrounds scattered arterioles.			9
216	Moderate numbers of lymphocytes, neutrophils and histiocytes infiltrate portal zones and accumulate in sinusoidal spaces. Scattered individual hepatocytes are degenerate/necrotic and are surrounded by aggregates of neutrophils and lymphocytes.	Hyperplastic splenic follicles.	Esophagus: aggregates of neutrophils multifocally widen the			9
247	Moderate numbers of lymphocytes, neutrophils and histiocytes infiltrate portal zones (liver) and accumulate in sinusoidal spaces. Scattered individual hepatocytes are degenerate/necrotic and are surrounded by aggregates of neutrophils and lymphocytes.	Hyperplastic splenic follicles	Small numbers of neutrophils are within scattered alveoli			9

www.manaraa.com

Mouse no.	Liver	Spleen	Lung	Kidney	Brain	Day Post Infection
248	Moderate numbers of lymphocytes, neutrophils and histiocytes infiltrate portal zones (liver). Widely scattered individual hepatocytes are degenerate/necrotic and are surrounded by small numbers of neutrophils or lymphocytes.	Hyperplastic splenic follicles with increased numbers of neutrophils.	Lymphocytic/neutrophilic myocarditis(section of heart accompanying lung). Heavy infiltrate of lymphocytes and histiocytes with fewer neutrophils in fat around heart and adjacent segments of pleurae. A large aggregate of pyogranulomatous inflammation replaces a group of alveoli (lung)			**9**
217	Moderate numbers of lymphocytes, neutrophils and histiocytes infiltrate portal zones (liver) and accumulate in sinusoidal spaces. Scattered individual hepatocytes are degenerate/necrotic and are surrounded by aggregates of neutrophils and lymphocytes.	Hyperplastic splenic follicles with scattered lytic cells and interstitial fibrin.	Esophagus: aggregates of neutrophils multifocally widen the submucosa. Neutrophils and histiocytes infiltrate periesophageal connective tissue unilaterally.			**10**
218	Moderate numbers of lymphocytes, neutrophils and histiocytes infiltrate portal zones (liver) and accumulate in sinusoidal spaces. Scattered individual hepatocytes are degenerate/necrotic and are surrounded by aggregates of neutrophils and lymphocytes.	Hyperplastic splenic follicles with regularly scattered lytic cells.	Scattered perivascular and peribronchiolar hemorrhages. Some larger vessels are also surrounded by moderate numbers of lymphocytes and neutrophils.			**10**

www.manaraa.com

Mouse no.	Liver	Spleen	Lung	Kidney	Brain	Day Post Infection
249	Moderate numbers of lymphocytes, neutrophils and histiocytes infiltrate portal zones (liver) and accumulate in sinusoidal spaces. Scattered individual hepatocytes are degenerate/necrotic and are surrounded by aggregates of neutrophils and lymphocytes.	Hyperplastic splenic follicles with regularly scattered lytic cells.	Scattered perivascular and peribronchiolar hemorrhages.			**10**
250	Moderate numbers of lymphocytes, neutrophils and histiocytes infiltrate portal zones (liver) and accumulate in sinusoidal spaces. Scattered individual hepatocytes are degenerate/necrotic and are surrounded by aggregates of neutrophils and lymphocytes.	Hyperplastic splenic follicles with scattered lytic cells	Mild neutrophilic/lymphocytic pleuritis.			**10**
300	Moderate numbers of lymphocytes, neutrophils and histiocytes infiltrate portal zones (liver) and small clusters accumulate in sinusoidal spaces. Scattered individual hepatocytes are degenerate/necrotic and are surrounded by aggregates of neutrophils and lymphocytes.	Hyperplastic splenic follicles with scattered lytic cells and interstitial fibrin.				**10**

www.manaraa.com

Mouse no.	Liver	Spleen	Lung	Kidney	Brain	Day Post Infection
237 Sham						**7**
238 Sham						**8**
239 Sham						**9**
240 Sham			Scattered perivascular and peribronchiolar hemorrhages			**10**

www.manaraa.com